(12) INTERNATIONAL APPLICATION PUBLISHED UNDER THE PATENT COOPERATION TREATY (PCT)

(19) World Intellectual Property Organization
International Bureau

(43) International Publication Date
14 July 2016 (14.07.2016)

(10) International Publication Number
WO 2016/110862 A1

(51) International Patent Classification:
H01M 4/24 (2006.01) *H01M 4/36* (2006.01)
H01M 4/26 (2006.01)

(21) International Application Number:
PCT/IN2015/000006

(22) International Filing Date:
6 January 2015 (06.01.2015)

(25) Filing Language: English

(26) Publication Language: English

(71) Applicant: **INDIAN INSTITUTE OF SCIENCE** [IN/IN]; Sir C V Raman Road, Malleswaram, Bangalore 560 012 (IN).

(72) Inventors: **ASHOK KUMAR, Shukla**; Indian Institute Of Science, Malleswaram, Bangalore 560012 (IN). **SRINIVASAN, Sampath**; Indian Institute Of Science, Malleswaram, Bangalore 560012 (IN). **ARAVAMUTHAN, Sundar Rajan**; Indian Institute Of Science, Malleswaram, Bangalore 560014 (IN).

(74) Agent: **SURESH, Jallipeta**; No. 46, FIRST CROSS, MARAPPA GARDEN, Benson Town Post, Bangalore 560046 (IN).

(81) Designated States *(unless otherwise indicated, for every kind of national protection available)*: AE, AG, AL, AM, AO, AT, AU, AZ, BA, BB, BG, BH, BN, BR, BW, BY, BZ, CA, CH, CL, CN, CO, CR, CU, CZ, DE, DK, DM, DO, DZ, EC, EE, EG, ES, FI, GB, GD, GE, GH, GM, GT, HN, HR, HU, ID, IL, IN, IR, IS, JP, KE, KG, KN, KP, KR, KZ, LA, LC, LK, LR, LS, LU, LY, MA, MD, ME, MG, MK, MN, MW, MX, MY, MZ, NA, NG, NI, NO, NZ, OM, PA, PE, PG, PH, PL, PT, QA, RO, RS, RU, RW, SA, SC, SD, SE, SG, SK, SL, SM, ST, SV, SY, TH, TJ, TM, TN, TR, TT, TZ, UA, UG, US, UZ, VC, VN, ZA, ZM, ZW.

(84) Designated States *(unless otherwise indicated, for every kind of regional protection available)*: ARIPO (BW, GH, GM, KE, LR, LS, MW, MZ, NA, RW, SD, SL, ST, SZ, TZ, UG, ZM, ZW), Eurasian (AM, AZ, BY, KG, KZ, RU, TJ, TM), European (AL, AT, BE, BG, CH, CY, CZ, DE, DK, EE, ES, FI, FR, GB, GR, HR, HU, IE, IS, IT, LT, LU, LV, MC, MK, MT, NL, NO, PL, PT, RO, RS, SE, SI, SK,

[Continued on next page]

(54) Title: GRAPHITE-GRAFTED ALKALINE IRON ELECTRODE

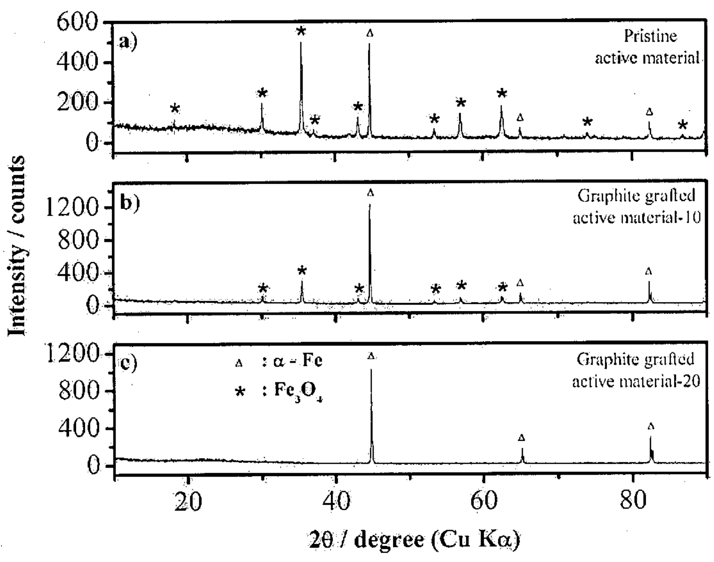

FIG.1

(57) Abstract: The present invention provides graphite-grafted alkaline iron electrode for an accumulator that renders a substantial amount of metallic iron (α-Fe) with an improved electrochemically active surface area and with substantially reduced oxide content (Fe_3O_4) of iron. The subject matter of the present invention also provides a method for the manufacture of graphite-grafted alkaline iron electrode for an accumulator in which graphite is grafted in situ into the active material, while decomposing a metal oxalate precursor in the presence of an organic carbon source.

WO 2016/110862 A1

SM, TR), OAPI (BF, BJ, CF, CG, CI, CM, GA, GN, GQ, GW, KM, ML, MR, NE, SN, TD, TG).

Declarations under Rule 4.17:

— *as to the identity of the inventor (Rule 4.17(i))*

— *as to applicant's entitlement to apply for and be granted a patent (Rule 4.17(ii))*

Published:

— *with international search report (Art. 21(3))*

GRAPHITE-GRAFTED ALKALINE IRON ELECTRODE

Field of invention

[001] The present invention relates to an alkaline iron electrode more particularly to a graphite-grafted alkaline iron electrode that renders a substantial amount of metallic iron (α-Fe) with an improved electrochemically active surface area and with substantially reduced oxide content (Fe_3O_4) of iron. The present invention also relates to a method of preparing a graphite-grafted alkaline iron electrode.

Background of the invention

[002] Iron is fourth most abundant element on the earth. It is cost effective, has large theoretical specific capacity and is non-toxic. Accordingly, there is an increased interest in developing iron-based accumulators. Iron-based accumulators are both mechanically and electrically rugged. Besides, iron electrodes are environmentally benign unlike other battery electrode materials such as cadmium, lead, nickel and zinc.

[003] The charge-discharge reactions of an alkaline iron electrode are given below. During the first charge-discharge step Fe (II) is reduced to Fe and vice versa as shown in reaction (1).

$$Fe + 2OH^- \leftrightarrows Fe(OH)_2 + 2e^- \qquad E° = -0.88 \text{ V vs. SHE} \qquad (1)$$

[004] The theoretical specific discharge capacity for the first step happens to be961 mAh/g. This step is followed by oxidation of Fe(II) to Fe(III) as depicted in reaction (2).

$$Fe(OH)_2 + OH^- \leftrightarrows FeOOH + H_2O + e^- \qquad E° = -0.56 \text{ V vs. SHE} \qquad (2)$$

[005] In reactions (1) and (2), E° is the standard reduction potential for the respective reactions and SHE stands for the standard hydrogen electrode. The open-circuit potential of a charged alkaline iron electrode (E° = - 0.88 V vs. SHE) is always more negative than the hydrogen evolution reaction in the same solution. Consequently, iron is thermodynamically unstable and suffers corrosion through concomitant evolution of hydrogen according to the reaction (3).

$$2H_2O + 2e^- \leftrightarrows H_2 + 2OH^- \qquad E^\circ = -0.83 \text{ V vs. SHE} \qquad (3)$$

[006] Dissolved oxygen in alkaline solution could also lead to the following reduction reaction during the corrosion of the iron electrode as depicted by reaction (4).

$$O_2 + 2\,H_2O + 4e^- \rightarrow 4\,OH^- \qquad E^\circ = 0.41 \text{ V vs. SHE} \qquad (4)$$

[007] As a result of these reactions, alkaline iron electrodes undergo a self-discharge of about 1–2% of their nominal capacity per day at 25°C. Hydrogen evolution also occurs while charging the alkaline iron electrodes and brings about a decrease in the charge acceptance. The degree of utilization of an alkaline iron electrode, based on reaction (1), varies from about 30% for electrodes of commercially pure iron to 60% for those made from high-purity iron. The faradaic efficiency of the iron electrode is reportedly increased by addition of bismuth sulphide (Bi2S3) that increases the hydrogen overpotential and hence the charge acceptance of the iron electrode.

[008] US2011/0236747A1 discloses an iron active material derived from ferrous oxalate dihydrate precursor to yield 15 w/w % α-Fe and 85 w/w % Fe_3O_4 with a specific discharge capacity of about 220 mAh/g at the current density of 40 mA/g. The low specific discharge capacity of the iron electrode is apparently due to the lower content of α-Fe.

[009] PCT/US2012/042750 discloses an iron electrode derived from carbonyl iron powder with specific discharge capacity of about 300 mAh/g, at about C/10 rate.

[010] US4250236 discloses an iron electrode derived from carbonyl iron powder with zinc sulphide additive that exhibits a specific discharge capacity of 370 mAh/g.

[011] A publication titled, "Self-Assembled Monolayers of n-Alkanethiols suppress Hydrogen Evolution and Increase the Efficiency of Rechargeable Iron Battery Electrodes", by Souradip Malkhandi *et al.,* in Journal of American Chemical Society 2013, 135, 347–353, discloses the effect of n-Alkanethiols in suppressing hydrogen evolution on Iron electrode and reports a specific discharge capacity of 300 mAh/g.

[012] A publication titled "Understanding the Factors Affecting the Formation of Carbonyl Iron Electrodes in Rechargeable Alkaline Iron Batteries", by Aswin K. Manohar *et al.,* in the Journal of The Electrochemical Society 159 (12) A2148-A2155 (2012), discloses the effect of wetting agent, pore former and sulphide additives on the formation of carbonyl iron electrodes.

[013] A publication titled, "An ultrafast nickel–iron battery from strongly coupled inorganic nanoparticle/nanocarbon hybrid materials", by Hailiang Wang *et al.,* in Nature Communications 3:917 doi: 10.1038/ncomms1921 (2012), discloses the ultra-fast Ni-Fe battery with FeOx nanoparticles grown on reduced graphene oxide and $Ni(OH)_2$ nanoplates grown on oxidized MWNT (Multi Wall Carbon Nanotubes) that exhibit a specific discharge capacity of 102 mAh/g at 37 A/g.

[014] The effect of various polymeric binders on the electrochemical performance and stability of the iron electrode are disclosed in a publication titled, "Effect of binder materials on cycling performance of Fe_2O_3 electrodes in alkaline solution", by Hiroki Kitamura et al., in the Journal of Power Sources 208 (2012) 391–396.

[015] In a publication titled "The role of FeS and (NH4)2CO3 additives on the pressed type Fe electrode", by Caldas *et al.,* in the Journal of Power Sources 74(1998) 108–112, discloses the effect of sulphide additive and pore forming agent on the performance of the iron electrode.

[016] A publication titled, "Formation mechanism of porous alkaline iron electrodes", by K. Vijayamohanan *et al.,* in Journal of power sources 32 (1990) 329-339 discloses iron electrodes with specific discharge capacities of about 300 mAh/g that have employed ferrous oxalate dihydrate as the precursor for the active material and FeS as faradaic efficiency agent.

[017] Therefore, there is a need to provide an alkaline iron electrode having a substantial amount of metallic iron and a reduced amount of corresponding oxide content of iron. There is also a need to provide an alkaline iron electrode that can effectively impart an increased specific discharge capacity, a reduced hydrogen evolution and increased charge-discharge cycles.

Objects of the present invention

[018] The primary object of the present invention is to provide a graphite-grafted alkaline iron electrode for an accumulator incorporating a substantial amount of metallic iron with an improved electrochemically active surface area and with a substantially reduced amount of corresponding oxide content of iron.

[019] An object of the present invention is to provide a graphite-grafted alkaline iron electrode for an accumulator having a graphitic carbon coated material with an optimum porosity.

[020] It is also an object of the present invention to provide a graphite-grafted alkaline iron electrode for an accumulator in which a parasitic reaction resulting in hydrogen evolution is mitigated.

[021] Another object of the present invention is to provide a graphite-grafted alkaline iron electrode for an accumulator with an increased specific discharge capacity.

[022] Still another object of the present invention is to provide a graphite-grafted alkaline iron electrode for an accumulator that imparts increased number charge-discharge cycles.

[023] It is also an object of the present invention to provide a method for the preparation of alkaline iron electrode for an accumulator, in which graphite is grafted in situ into the active material (a mixture of α-Fe and Fe_3O_4), while decomposing a metal oxalate precursor, in the presence of an organic carbon source.

[024] These and the other objects and the appurtenant advantages of the embodiments herein will be understood easily by studying the following specification with the accompanying drawings.

Summary of the invention

[025] The present invention provides a graphite-grafted alkaline iron electrode for an accumulator having an increased amount of metallic iron (α-Fe) concomitant to substantially reduced amount of oxide of iron (Fe_3O_4). The active material in the iron electrode is grafted with graphite through an organic carbon source, preferably polyvinyl alcohol. The iron electrode also includes an additive to inhibit hydrogen evolution, a conductive carbon having a high surface-area-to-volume ratio and a metal salt. The active material in the alkaline iron electrode of the present invention is provided with a graphitic carbon coated particles that imparts an increased specific discharge capacity along with a faradaic efficiency of about 80%. The present invention also provides a method to prepare graphite-grafted alkaline iron electrode for an accumulator in which graphite is grafted in situ into the active material, while decomposing a metal oxalate precursor along with an organic carbon source.

Brief description of the drawings

[026] **FIG.1a, FIG.1b** and **FIG.1c** are powder X-ray diffractograms for pristine active material obtained by decomposing ferrous oxalate dihydrate (α-$FeC_2O_4.2H_2O$) (1a) and for graphite-grafted active materials (GGAM-10 and GGAM-20) obtained by decomposing α-$FeC_2O_4.2H_2O$–10 w/w % Polyvinyl alcohol (PVA) composite (1b) and α-$FeC_2O_4.2H_2O$–20 w/w % Polyvinyl alcohol (PVA) composite (1c)(International Centre for Diffraction Data (ICDD) number for α-Fe and Fe_3O_4 are 00-006-0696 and 00-019-0629, respectively).

[027] **FIG.2** shows galvanostatic charge and discharge data for alkaline iron electrode made from pristine active material and graphite-grafted active material (GGAM-10) at charge and discharge current density of 100mA/g.

[028] **FIG.3** shows the first derivative of charging potential (V) with respect to charge capacity (Q) as a function of charge capacity (Q) for iron electrode derived from pristine active material and graphite-grafted active material (GGAM-10) of the present invention.

[029] **FIG.4** shows the Nyquist plots obtained for iron electrodes made from pristine active material and graphite-grafted active material (GGAM-10) of the present invention.

[030] **FIG.5** is the powder X-ray diffraction pattern for graphitic carbon extracted from graphite-grafted active material (GGAM-10) after reacting with 5 M HCl.

[031] **FIGs.6a, FIG.6b** and **FIG.6c** are Raman spectra for pristine active material, graphite-grafted active material (GGAM-10) and for graphitic carbon extracted from graphite-grafted active material (GGAM-10), respectively.

[032] **FIG.7** shows the data for the specific discharge capacity of iron electrode made from graphite-grafted active material with varying PVA content in the precursor composite (in w/w %).

[033] **FIG.8** shows the data for the specific discharge capacity of iron electrode made from pristine active material without Bi_2S_3, pristine active material with Bi_2S_3 and graphite-grafted active material (GGAM-10) of the present invention with Bi_2S_3.

[034] **FIG.9a** and **FIG.9b** are powder X-ray diffraction patterns for Bi_2S_3 additive and elemental Bi formed electrochemically by the reduction of Bi_2S_3 (International Centre for Diffraction Data (ICDD) number for Bi_2S_3: 00-017-0320 and for Bi: 00-044-1246).

[035] **FIG.10a** shows the data for the specific discharge capacity of iron electrode made from graphite-grafted active material (GGAM-10) at varying discharge rates.

[036] **FIG.10b** depicts the bench test results of the iron electrodes made from graphite-grafted active material (GGAM-10) of the present invention.

[037] **FIG.11** shows the data for the specific discharge capacity for iron electrode made from graphite-grafted active material (GGAM-10) at varying temperatures.

[038] **FIG.12a** and **FIG.12b** are Field Emission Scanning Electron Microscopic (FESEM) images for pristine active material and graphite-grafted active material (GGAM-10) of the present invention.

[039] **FIG.13** shows FESEM images for Bi_2S_3 additive used in the iron electrode.

[040] **FIG.14** is a flow chart depicting process steps for the preparation of α-$FeC_2O_4.2H_2O$ (precursor for pristine and graphite-grafted active material).

[041] **FIG.15** is a flow chart depicting process steps for the preparation of pristine active material.

[042] **FIG.16** is a flow chart depicting process steps for the preparation of graphite-grafted active material.

[043] **FIG.17** is a flow chart depicting process steps for the preparation of Iron electrode with graphite-grafted active material of the present invention.

Detailed description of the invention

[044] The following is a detailed description of graphite-grafted alkaline iron electrode for an accumulator according to the present invention.

[045] The invention is characterized by a graphite-grafted alkaline iron electrode for an accumulator comprising as its principal ingredient, a substantial amount of metallic iron with an enhanced surface area, an optimum porosity and with a substantially reduced amount of corresponding oxide content, to impart an increased specific discharge capacity and an improved faradaic efficiency.

[046] The graphite-grafted alkaline iron electrode of the present invention comprises approximately 80-95 w/w % of metallic iron (α-Fe), 5-20 w/w % of oxide content (Fe_3O_4). The graphite-grafted active material is provided with an enhanced surface area in the range of 10-15 m^2/g.

[047] In an aspect of the present invention the graphite-grafted active material of the graphite-grafted alkaline iron electrode of the present invention is provided with a desired porous structure, having mean pore-diameter in the range of 8-15 nm.

[048] The graphite-grafted alkaline iron electrode of the present invention includes graphitic carbon in the range of about 2-3 w/w %. The graphitic carbon is formed from the organic carbon source, selected from polyvinyl alcohol, resorcinol-formaldehyde resin, sucrose and starch. In the present invention, as a preferred embodiment polyvinyl alcohol is used as an organic carbon source for the graphite-grafted alkaline iron electrode. Polyvinyl alcohol (PVA) acts not only as a reducing agent but also as a graphitic carbon source. The incorporation of the graphitic carbon derived from the selected organic carbon source imparts a reduction in internal resistance of the material by imparting electronically-wired architecture.

[049] In another aspect of the present invention, the electrode exhibits improved conductivity with increased charge acceptance, due to the incorporation of graphitic carbon derived from the organic carbon source such as polyvinyl alcohol along with the precursor.

[050] In another aspect of the present invention, a conductive carbon with high surface-area-to-volume ratio, preferably carbon black is incorporated in desired quantities for imparting an enhanced electrical conductivity. In this invention, advantageously, carbon black is used in the range of about 10-20 w/w %.

[051] In yet another aspect of the present invention, the graphite-grafted alkaline iron electrode of the present invention includes a faradaic efficiency agent. The faradaic efficiency agent increases hydrogen overpotential and hence the charge acceptance of the iron electrode. In a preferred embodiment bismuth sulphide (Bi_2S_3) is used as faradaic efficiency agent in the range of about 1-2 w/w %. The other suitable faradaic efficiency agents such as bismuth sulphide (Bi_2S_3), lead sulphide and ferrous sulphide, preferably bismuth sulphide can also be suitably used. The faradaic efficiency agent is used to improve coulombic efficiency and to inhibit kinetics of hydrogen evolution.

[052] The graphite-grafted alkaline iron electrode of the present invention further includes a metal salt such as nickel sulphate, in the range of about 1-2 w/w %.

[053] In another preferred aspect of the present invention the graphite-grafted alkaline iron electrode further comprises at least one binder such as polytetrafluoroethylene (PTFE), polyvinylidene fluoride (PVDF), styrene-butadiene-rubber (SBR), acrylic resin, hydroxypropyl-methyl-cellulose (HPMC), neoprene latex, polyethylene (PE), poly tetrafluoroethylene-co-vinylidene fluoride (P(TFE-VDF)) or a mixture thereof.

[054] In yet another aspect of the present invention polytetrafluoroethylene (PTFE), as a polymer binder, is used in the range of about 6-15 w/w%.

[055] The graphite-grafted alkaline iron electrode of the present invention with an increased amount of metallic iron content exhibits specific discharge capacity of about 400 mAh/g, at current density of 100 mA/g.

[056] In yet another aspect of the present invention the specific discharge capacity for the electrode of the present invention is about 33 % higher at the current density of 100mA/g as compared to the pristine active material.

[057] It is also an aspect of the present invention that the graphite-grafted alkaline iron electrode of the present invention displays specific discharge capacity values of about 375 mAh/g and 320 mAh/g, even at higher discharge rates like C and 2C rate.

[058] Now specifically referring to **FIG.1a**, **FIG.1b** and **FIG.1c**, of the accompanied drawings that depict XRD patterns for pristine active material and graphite-grafted active material (GGAM-10 and GGAM-20) of the present invention, respectively. The diffraction lines corresponding to α-Fe and Fe_3O_4 are indicated in the XRD patterns as Δ for α-Fe and * for Fe_3O_4. For graphite-grafted active materials, the relative intensity of the diffraction lines corresponding to Fe_3O_4 reduces as the amount of PVA in the precursor composite increases; when the PVA content in the precursor composite is 20 w/w %, the diffraction pattern suggest the absence of Fe_3O_4. The diffraction data suggests an increase in the relative intensity of the diffraction lines corresponding to α-Fe with increase in the amount of PVA in the precursor composite. The following steps occur while preparing the graphite-grafted active material:(i) α-$FeC_2O_4.2H_2O$–PVA composite to α-FeC_2O_4–PVA composite i.e., dihydrate to anhydrous compound, (ii) thermal decomposition of α-FeC_2O_4 and PVA, (iii) carbonization of polymer (PVA), and (iv) reduction of Fe_3O_4 (magnetite) to α-Fe (metallic iron) by carbonaceous products. Besides, about 2–3 w/w % of graphitic carbon is obtained as a conductive coating on the surface of the iron and magnetite particles. Accordingly, PVA acts both as a reducing agent and graphitic-carbon source.

[059] Referring to **FIG.2**, which is plot depicting galvanostatic charge and discharge profiles for alkaline iron electrode with pristine active material and graphite-grafted active material (GGAM-10) of the present invention. It is seen from **FIG.2**, that graphite-grafted alkaline iron electrode of the present invention with Bi_2S_3 additive, exhibits a specific discharge capacity of about 400 mAh/g (at C/4 rate or 100 mA/g) with a faradaic efficiency of about 80% as compared to the specific discharge capacity of 300 mAh/g at 100 mA/g with a faradaic efficiency of about 60% obtained for pristine active material with Bi_2S_3 additive. In this exemplary embodiment, the current density value for both charge and discharge processes are maintained at 100 mA/g. The charging potential profiles for iron electrode follow an S-shaped curve with two plateaus at -1.1 V vs. mercury/mercuric oxide (MMO) and -1.15 V vs. MMO. It can be observed here that the hydrogen evolution is higher for the second plateau potential at -1.15 V vs. MMO compared to the first plateau potential at -1.1 V vs. MMO since the former is about 50mV more negative. In the case of pristine active material, the electrode potential reaches the second plateau after accepting a charge of about 320 mAh/g, but in the case of graphite-grafted active material, the electrode potential reaches the second plateau after accepting a charge of about 450 mAh/g. Graphite-grafted active material of the present invention shows an increased charge acceptance due to the presence of higher amount of metallic iron. Besides, in the discharge potential profile, the initial potential drop is lesser for graphite-grafted active material compared to pristine active material due to the presence of graphitic carbon coating and an increased amount of metallic iron.

[060] In another aspect of the present invention, referring to **FIG.3**, the first derivative of charging potential (V) with respect to charge capacity (Q) is plotted against charge capacity (Q) for iron electrode derived from pristine active material and graphite-grafted active material (GGAM-10) of the present invention. The charging potential profile of iron electrode has an inflection region. The derivative plot clearly shows the inflection region as peak. For pristine active material, a peak centered at nearly 270 mAh/g is observed, while a peak at 430 mAh/g is observed for graphite-grafted active material of the present invention. Accordingly, there is an increase in charge acceptance for graphite-grafted active material of the present invention, due to the increase in the amount of metallic iron present in the material.

[061]` In a further aspect of the present invention, the Nyquist plots for iron electrode comprising pristine active material and graphite-grafted active material (GGAM-10) of the present invention are shown in **FIG.4**. The inset depicts the magnified image in the high-frequency region. Electrochemical Impedance data for the cell are obtained at fully-charged state at open-circuit potential in the frequency range between 100 kHz and 100 mHz with an AC amplitude of 5 mV. At –Z'' = 0, the Z' value corresponds to the ohmic resistance of the electrode material, electrolyte and current collector. The ohmic resistance for iron electrode with graphite-grafted active material of the present invention is 32 mΩ, which is lower in relation to 41.5 mΩ for pristine active material, due to the presence of increased amount of metallic iron in the former.

[062] Now, referring to **FIG.5**, which is a powder XRD pattern for graphitic carbon extracted from the graphite-grafted active material (GGAM-10) of the present invention, by etching α-Fe and Fe_3O_4 with 5M HCl. As a result, iron and magnetite go into solution as chlorides of iron. Thereafter, about 2 w/w % of carbon is found to be present in the graphite-grafted active material of the present invention, which is determined by filtering out the iron chlorides in the solution and weighing the residual carbon. Broad peaks that are typical to graphitic carbon are observed in the XRD pattern.

[063] In another aspect of the present invention, in order to ascertain the presence of graphitic carbon in the graphite-grafted active material, Raman spectral analysis is performed and the corresponding spectra are shown in **FIG.6a**, **FIG.6b** and **FIG.6c**. **FIG. 6a**, depicts the Raman spectrum of the pristine active material where no graphitic carbon is present. **FIG.6b** depicts the Raman spectrum of the graphite-grafted active material (GGAM-10) and the spectrum clearly reveals the presence of graphitic carbon. **FIG.6c** shows the Raman spectrum of the graphitic carbon extracted from graphite-grafted active material (GGAM-10) by treating it with 5M HCl to remove the metallic iron and Fe_3O_4 and the spectrum further affirms the presence of graphitic carbon. The Raman spectra (excitation wavelength=514nm) for graphite-grafted active material (GGAM-10)(**FIG. 6b**) and the metal and metal oxide etched out material (graphitic carbon) (**FIG.6c**) of the present invention, reveal two broad bands, one at 1592 cm^{-1} assigned to the E_{2g} mode of graphite, and the other centered at 1352 cm^{-1} assigned to the disorder-induced peak characteristic of highly defective graphite present in the material.

[064] In another aspect of the present invention, in order to determine an optimum amount of PVA in the precursor, which is required for graphite-grafted active material, the specific discharge capacity for graphite-grafted active material of the present invention with varying amounts of PVA in the precursor are determined and shown in **FIG.7**. It is observed here that graphite-grafted active material with about 10 w/w % of PVA is optimum, to deliver a specific discharge capacity of 400 mAh/g at C/4 rate.

[065] In yet another aspect of the present invention, the specific discharge capacities for the iron electrode made from graphite-grafted active material (GGAM-10) of the present invention along with a faradaic efficiency agent such as Bi_2S_3 and pristine active material with and without Bi_2S_3 additive as a function of cycle number are shown in **FIG.8**. For graphite-grafted active material of the present invention along with Bi_2S_3 additive, a specific discharge capacity of about 386 mAh/g at 100 mA/g is obtained, which recedes to a specific discharge capacity of 356 mAh/g at 100th cycle. For pristine active material with Bi_2S_3 additive, a specific discharge capacity of 302 mAh/g at 100 mA/g is obtained, which recedes to a specific discharge capacity of 258 mAh/g at 100th cycle. In case of pristine active material without Bi_2S_3 additive, a specific discharge capacity of 145 mAh/g is obtained for 1st cycle that subsequently recedes to about 4 mAh/g. It is therefore surmised that faradaic efficiency agent Bi_2S_3 improves the charge acceptance of the iron electrode by increasing the hydrogen over potential. It appears that, for pristine active material without Bi_2S_3 additive, the initial specific discharge capacity of 145 mAh/g is obtained for the first cycle due to the presence of α-Fe in the pristine active material but in the subsequent cycle hydrogen evolution dominates preventing the conversion of oxidized iron to metallic iron that restricts its capacity. In the case of pristine active material and graphite-grafted active material with Bi_2S_3 additive, elemental bismuth is formed from Bi_2S_3 on the surface of the electrode material following the reaction:

$$Bi_2S_3 + 6e^- \leftrightarrows 2Bi + 3S^{2-} \qquad E^o = -0.82 \text{ V vs. SHE} \qquad (5)$$

[066] The above aspect is further substantiated by the powder XRD of Bi_2S_3 additive used in the iron electrode and the elemental Bi formed electrochemically in the iron electrode as shown in **FIG. 9**.

[067] The iron electrodes of the present invention are subjected to various rate charge and discharge (C/10, C/5, C/2, C and 2C rate) as shown in **FIG. 10a**. (C/n denotes the rate at which a full charge or discharge takes n hours, means C/2 rate discharge takes 2h to complete and C rate discharge takes 1h to complete). At C/10, C/5, C/2 rate, a specific discharge capacity of 400 mAh/g is obtained with a faradaic efficiency of about 80%. Even at C and 2C rate, a specific discharge capacity of 376 and 322 mAh/g are obtained with a faradaic efficiency of 75 and 64%. These iron electrodes take 10-15 charge-discharge cycles to reach a stable specific discharge capacity, which is termed as formation cycles. After formation cycles, these electrodes are tested at various charge-discharge rates as shown in **FIG.10b** and the corresponding values are summarized in **Table 1**.

Table 1

Charge and discharge rate	Charge and discharge current density (mA/g)	Specific discharge capacity (mAh/g)	Faradaic efficiency (%)
C/10	40	400	80
C/5	80	410	82
C/2	190	403	81
C	360	376	75
2C	620	322	64

[068] In another aspect of the present invention, the discharge potential profiles for iron electrode comprising graphite-grafted active material (GGAM-10) of the present invention, with 10 w/w % PVA in the precursor at varying temperatures, at C/5 rate, are shown in the **FIG.11**.

[069] In yet another aspect of the present invention, Field Emission Scanning Electron Microscopic (FESEM) images for the pristine active material and graphite-grafted active material of the present invention are shown in **FIG.12a** and **FIG.12b**. **FIG.12a** and **FIG.12b** are the images of the active material of the present invention without and with PVA in the precursor, exhibiting cuboidal particles of 5-10 microns.

[070] FESEM images for the Bi_2S_3 additive used in the iron electrodes are shown in **FIG.13**.

[071] In an aspect of the present invention, the process for the preparation of graphite-grafted alkaline iron electrode for an accumulator, comprises the steps of preparing ferrous oxalate dihydrate (α-$FeC_2O_4.2H_2O$) from $FeSO_4.7H_2O$ and oxalic acid dihydrate, which is followed by grafting of graphite *in situ*, by decomposing ferrous oxalate dihydrate, at a temperature in the range of 550-650°C in vacuum and in the presence of an effective amount of organic carbon source. A faradaic efficiency agent and carbon black added to the graphite-grafted active material. This material is compacted and cured in the presence of a binder at a temperature of about 350°C, in an inert atmosphere, to obtain alkaline iron electrode having a substantial amount of metallic iron and a substantially reduced amount of oxide of iron.

[072] The various steps of the process for the preparation of graphite-grafted alkaline iron electrode for an accumulator of the present invention are now described in detail, by referring to flow-drawings as shown in **FIGs. 14-17**.

Preparation of α-$FeC_2O_4.2H_2O$ (precursor for active material)

[073] A solution of an iron source is prepared by dissolving the iron source in hot and de-ionized water at a temperature in the range of 60-80°C, preferably at about 70°C. In the process of the present invention, the iron source that is advantageously used is ferrous sulphate heptahydrate ($FeSO_4.7H_2O$). It is understood here that other iron sources such as hydrated ferrous ammonium sulphate ($(NH4)2Fe(SO_4)_2.6H_2O$) and hydrated iron chloride

($FeCl_2.2H_2O$) can also be suitably used as precursors for the process. Thus a solution of ferrous sulphate heptahydrate ($FeSO_4.7H_2O$) is prepared. A suitable dicarboxylic acid is selected and a solution of the same is also prepared. A solution of dicarboxylic acid is prepared by dissolving the selected dicarboxylic acid in de-ionized water at a temperature in the range of 60-80°C, preferably at about 70°C. Advantageously, in the present invention, as an exemplary embodiment, oxalic acid dihydrate ($H_2C_2O_4.2H_2O$) is used for preparing the desired dicarboxylic acid solution. The other dicarboxylic acids that can be suitably used are malonic acid, succinic acid and adipic acid. The oxalic acid dihydrate ($H_2C_2O_4.2H_2O$), solution thus prepared is slowly added into ferrous sulphate solution under continuous stirring at a temperature in the range of about 60 to 70°C to precipitateα-ferrous oxalate dihydrate (α-$FeC_2O_4.2H_2O$). The precipitated α-$FeC_2O_4.2H_2O$ is allowed for ageing along with the supernatant liquid for about two hours, allowing the precipitate to settle down, followed by filtration. The filtered product is dried in air oven at a temperature in the range of 60-70°C.

Preparation of graphite-grafted active material

[074] A composite is prepared by mixing an organic carbon source, such as Polyvinyl Alcohol (PVA) of desired molecular weight with α-Ferrous oxalate dihydrate (α-$FeC_2O_4.2H_2O$). In this process PVA is advantageously used as the organic carbon source. However, other organic carbon sources such as resorcinol-formaldehyde resin, sucrose and starch can also be suitably used. The composite is initially heated to about 200°C and maintained at that temperature for about one hour, for converting α-$FeC_2O_4.2H_2O$-PVA composite to α-FeC_2O_4-PVA composite, which is an anhydrous compound. Subsequently, the α-FeC_2O_4-PVA composite is heated to about 400°C and maintained at that temperature for about one hour. Finally, the temperature is increased to about 600°C and maintained for about two to three hours to obtain graphite-grafted active material (GGAM), which is a mixture of graphitic carbon coated α-Fe and Fe_3O_4. The carbonaceous material, which gets formed while decomposing PVA, reduces Fe_3O_4 to α-Fe (metallic iron). The graphite-grafted active material thus obtained comprises porous cuboidal particles of α-Fe and Fe_3O_4, where the particle size is of the material is in the range of 5-10 microns (μm).

Preparation of iron electrode

[075] A pore forming agent is prepared by adding a solution of $NiSO_4$ to an alkali solution, advantageously KOH solution, in order to obtain a colloidal $Ni(OH)_2$ precipitate. Then active material, carbon black and Bi_2S_3 are added in a proportion in the range of 82.5:10:1 by mass into the solution. These components are mixed homogeneously and the slurry is obtained. To this slurry a polymeric binder, advantageously polytetrafluoroethylene (PTFE) is added. After adding PTFE into the mixture, dough is formed. It is spread over a degreased nickel mesh of desired dimensions and compacted under pressure to form compressed electrodes. The compressed electrodes are cured at a temperature of 350°C, in an inert atmosphere such as N2 atmosphere for about 40 minutes, to obtain the negative iron electrode.

[076] The preferred embodiments of the subject matter of the invention are now described in the form of the following examples, which are exemplary and non-limiting in nature and shall not be construed as limiting the scope of the present invention.

Example 1

[077] In the first step, 109 g of ferrous sulphate heptahydrate ($FeSO_4.7H_2O$) is dissolved in 400 mL of hot de-ionized water (about 70°C) and then 54 g of oxalic acid dihydrate ($H_2C_2O_4.2H_2O$) is dissolved in 400 mL of hot de-ionized water (about 70°C). In order to avoid oxidation of ferrous ion in the solution by dissolved oxygen, nitrogen gas is bubbled for 10-15 minutes in to the de-ionized water prior to the experiments. Then oxalic acid solution is slowly added in to ferrous sulphate solution with continuous stirring at about 70°C and the α-ferrous oxalate dihydrate (α-$FeC_2O_4.2H_2O$) gets precipitated. The precipitated α-$FeC_2O_4.2H_2O$ is allowed for ageing along with the supernatant liquid for about 2 h at 70°C, filtered and dried in air oven at 60-70°C.

[078] In the second step, 10 g of α-$FeC_2O_4.2H_2O$ is first heated up to 200°C and maintained at that temperature for 1h for converting dihydrate to anhydrous compound. Subsequently, the anhydrous mass is heated to 400°C and maintained at that temperature for 1h in vacuum. Finally, the temperature is raised to 600°C and maintained for 2-3 h to obtain pristine active material, which is a mixture of α-Fe and Fe_3O_4.The powder XRD pattern and Raman spectrum of pristine active material are shown in **FIG.1a** and **FIG.6a**. The product comprises porous cuboidal particles of about 5-10 microns as shown in the **FIG.12a**.

[079] In the third step, 0.6 mL of 3.6 w/v % $NiSO_4$ solution is added in to 0.6 mL of 1 w/v % KOH solution, in order to obtain colloidal $Ni(OH)_2$ precipitate, which act as a pore forming agent. Then pristine active material, carbon black and Bi_2S_3 are added in a proportion of 82.5:10:1 by mass in to the solution. These components are mixed homogeneously and the slurry is obtained. Then 6 w/w % polymeric binder, namely polytetrafluoroethylene (PTFE) 60 wt. % dispersion in H_2O is added. After adding PTFE in to the mixture, dough is formed. It is spread over a degreased nickel mesh of dimension 3.1×3.3 cm^2 and compacted at 675 kg/cm^2. The compressed electrodes are cured at 350°C in N_2 atmosphere for 40 minutes to obtain the negative Iron electrode. 1g of pristine active material is distributed over an area of 17.4 cm^2 (pristine active material loading = 57.5 mg/cm^2). Subsequently, this negative electrode is assembled with nickel oxyhydroxide counter electrodes on either side with mercury/mercuric oxide (MMO) as a reference electrode ($E°= 0.098$ V vs. SHE) in 6 M KOH solution with 1 w/v % LiOH. Alkaline iron electrodes are subjected to galvanostatic charging and discharging at a current-density of 100 mA/g up to - 0.8 V vs. MMO during the first step of discharge. A maximum specific discharge capacity of 300 mAh/g is obtained at 100 mA/g current density with a faradaic efficiency of 60 % as shown in **FIG.2**. The (dV/dQ) vs. Q plot as shown in **FIG.3** implies that there is a poor charge acceptance for the pristine active material. The Nyquist plot as shown in **FIG.4** implies a higher ohmic resistance in the electrode material. The specific discharge capacity of iron electrode made from pristine active material with and without Bi_2S_3 as a function of cycle number is shown in **FIG.8**. The XRD pattern of Bi_2S_3 used in the iron electrode and elemental Bi, which is electrochemically reduced from Bi_2S_3 are shown in **FIG.9a** and **FIG.9b**. The FESEM images of Bi_2S_3 used in the electrodes are shown in **FIG.13**.

Example 2

[080] In the first step, 109 g of ferrous sulphate heptahydrate ($FeSO_4.7H_2O$) is dissolved in 400 mL of hot de-ionized water (about 70°C) and then 54 g of Oxalic acid dihydrate

($H_2C_2O_4.2H_2O$) is dissolved in 400 mL of hot de-ionized water (about 70°C). In order to avoid oxidation of ferrous ion in the solution by dissolved oxygen, nitrogen gas is bubbled for 10-15 minutes into the de-ionized water prior to the experiments. Then oxalic acid solution is slowly added in to ferrous sulphate solution with continuous stirring at about 70°C and the α-Ferrous oxalate dihydrate (α-$FeC_2O_4.2H_2O$) is precipitated. The precipitated α-$FeC_2O_4.2H_2O$is allowed for ageing along with the supernatant liquid for about 2 hours at 70°C, filtered and dried in air oven at 60-70°C.

[081] In the second step, 9.5 g of α-$FeC_2O_4.2H_2O$and 0.5 g of Polyvinyl Alcohol (PVA, Mw = 1, 25,000) are extensively mixed and the resultant composite is first heated up to 200°C and maintained at that temperature for 1h for converting α-$FeC_2O_4.2H_2O$-PVA composite to α-FeC_2O_4-PVA composite. Subsequently, the α- FeC_2O_4-PVA composite is heated to 400°C and maintained at that temperature for 1h. Finally, the temperature is raised to 600°C and maintained for 2-3 h to obtain graphite-grafted active material (GGAM-5), which is a mixture of graphitic carbon coated α-Fe and Fe_3O_4. The carbonaceous material, which gets formed while decomposing PVA, reduces a part of Fe_3O_4 to α-Fe (metallic iron). Here the decomposition is done under vacuum. The mixture comprises porous cuboidal particles of about 5-10 microns (μm).

[082] In the third step, 0.6 mL of 3.6 w/v % $NiSO_4$ solution is added in to 0.6 mL of 1 w/v % KOH solution, in order to obtain colloidal $Ni(OH)_2$ precipitate, which act as a pore forming agent. Then graphite-grafted active material (GGAM-5), carbon black and Bi_2S_3 are added in a proportion of 82.5:10:1 by mass in to the solution. These components are mixed homogeneously and the slurry is obtained. Then 6 w/w% polymeric binder, namely polytetrafluoroethylene (PTFE) 60 wt. % dispersion in H_2O is added. After adding PTFE in to the mixture, dough gets formed. It is spread over a degreased nickel mesh of dimension 3.1 × 3.3 cm^2 and compacted at 675 kg/cm^2. The compressed electrodes are cured at 350°C in N_2 atmosphere for 40 minutes to obtain the negative Iron electrode. 1g of graphite-grafted active material is distributed over an area of 17.4 cm^2 (graphite-grafted active material loading = 57.5 mg/cm^2). Subsequently, this negative electrode is assembled with nickel oxyhydroxide counter electrodes on either side with mercury/mercuric oxide (MMO) as a reference electrode (E°= 0.098 V vs. SHE) in 6 M KOH solution with 1 w/v % LiOH. Alkaline iron electrodes are subjected to galvanostatic charging and discharging at a current density of 100 mA/g up to - 0.8 V vs. MMO during the first step of discharge. A maximum specific discharge capacity of 354 mAh/g is obtained at 100 mA/g current density with a faradaic efficiency of 71 % as shown in **FIG.7**.

Example 3

[083] In the first step, 109 g of ferrous sulphate heptahydrate ($FeSO_4.7H_2O$) is dissolved in 400 mL of hot de-ionized water (about 70°C) and then 54 g of oxalic acid dihydrate ($H_2C_2O_4.2H_2O$) is dissolved in 400 mL of hot de-ionized water (about 70°C). In order to avoid oxidation of ferrous ion in the solution by dissolved oxygen, nitrogen gas is bubbled for 10-15 minutes in to the de-ionized water prior to the experiments. Then oxalic acid solution is slowly added in to ferrous sulphate solution with continuous stirring at about 70°C and the α-ferrous oxalate dihydrate (α-$FeC_2O_4.2H_2O$) gets precipitated. The precipitated α-$FeC_2O_4.2H_2O$ is allowed for ageing along with the supernatant liquid for about 2 hours at 70°C, filtered and dried in air oven at 60-70°C.

[084] In the second step, 9 g of α- $FeC_2O_4.2H_2O$ and 1 g of Polyvinyl Alcohol (PVA, Mw = 1, 25,000) are extensively mixed and the resultant composite is first heated up to 200°C and maintained at that temperature for 1h for converting α- $FeC_2O_4.2H_2O$ -PVA composite to α- $FeC_2O_4.2H_2O$-PVA composite. Subsequently, the α- $FeC_2O_4.2H_2O$-PVA composite is heated to 400°C and maintained at that temperature for 1h. Finally, the temperature is raised to 600°C and maintained for 2-3 hours to obtain graphite-grafted active material (GGAM-10), which is a mixture of graphitic carbon coated α-Fe and Fe_3O_4. The powder XRD pattern and Raman spectrum of graphite-grafted active material (GGAM-10) are shown in **FIG.1b** and **FIG.6b**. The carbonaceous material, which gets formed while decomposing PVA, reduces a part of Fe_3O_4 to α-Fe (metallic iron). Here the decomposition is done under vacuum. The mixture comprises porous cuboidal particles of about 5-10 microns as shown in the **FIG.12b**. The powder XRD pattern and Raman spectrum of graphitic carbon extracted from graphite-grafted active material (GGAM-10) are shown in **FIG.5** and **FIG.6c**.

[085] In the third step, 0.6 mL of 3.6 w/v % $NiSO_4$ solution is added in to 0.6 mL of 1 w/v % KOH solution, in order to obtain colloidal $Ni(OH)_2$ precipitate, which act as a pore forming agent. Then graphite-grafted active material (GGAM-10), carbon black and Bi2S3 are added in a proportion of 82.5:10:1 by mass in to the solution. These components are mixed homogeneously and the slurry is obtained. Then 6 w/w % polymeric binder, namely polytetrafluoroethylene (PTFE) 60 wt. % dispersion in H2O is added. After adding PTFE in to the mixture, dough is formed. It is spread over a degreased nickel mesh of dimension 3.1 × 3.3 cm^2 and compacted at 675 kg/cm^2. The compressed electrodes are cured at 350°C in N2 atmosphere for 40 minutes to obtain the negative Iron electrode. 1g of graphite-grafted active material is distributed over an area of 17.4 cm^2 (graphite-grafted active material loading = 57.5 mg/cm^2). Subsequently, this negative electrode is assembled with nickel oxyhydroxide counter electrodes on either side with mercury/mercuric oxide (MMO) as a reference electrode ($E°$= 0.098 V vs. SHE) in 6 M KOH solution with 1 w/v % LiOH. Alkaline iron electrodes were subjected to galvanostatic charging and discharging at a current-density of 100 mA/g up to - 0.8 V vs. MMO during the first step of discharge. A maximum specific discharge capacity of 410 mAh/g is obtained at 100 mA/g current density with a faradaic efficiency of 82 % as shown in **FIG.2** and **FIG.7**.The (dV/dQ) vs. Q plot as shown in **FIG.3** implies that there is an increase in charge acceptance. The Nyquist plot as shown in **FIG.4** implies a decreased ohmic resistance in the electrode material. The specific discharge capacity of iron electrode made from GGAM-10 as a function of cycle number is shown in **FIG.8**. The specific discharge capacity of iron electrode made from GGAM-10 as a function of discharge rate is shown in **FIG.10a** and **FIG.10b**. The specific discharge capacity as a function of temperature is shown in **FIG. 11**.

Example 4

[086] In the first step, 109 g of ferrous sulphate heptahydrate (FeSO4.7H2O) is dissolved in 400 mL of hot de-ionized water (about 70°C) and then 54 g of oxalic acid dihydrate ($H_2C_2O_4.2H_2O$) is dissolved in 400 mL of hot de-ionized water (about 70°C). In order to avoid oxidation of ferrous ion in the solution by dissolved oxygen, nitrogen gas is bubbled for 10-15 minutes in to the de-ionized water prior to the experiments. Then oxalic acid solution is slowly added in to ferrous sulphate solution with continuous stirring at about 70°C and the α-ferrous oxalate dihydrate (α-$FeC_2O_4.2H_2O$) gets precipitated. The precipitated α-$FeC_2O_4.2H_2O$ is allowed for ageing along with the supernatant liquid for about 2 hours at 70°C, filtered and dried in air oven at 60-70°C.

[087] In the second step, 8.5 g of α-$FeC_2O_4.2H_2O$ and 1.5 g of Polyvinyl Alcohol (PVA, Mw = 1, 25,000) are extensively mixed and the resultant composite is first heated up to 200°C and maintained at that temperature for 1h for converting α-$FeC_2O_4.2H_2O$-PVA composite to α-FeC_2O_4-PVA composite. Subsequently α-FeC_2O_4-PVA composite is heated to 400°C and maintained at that temperature for 1h. Finally, the temperature is raised to 600°C and maintained for 2-3 hrs to obtain graphite-grafted active material (GGAM-15), which is a mixture of graphitic carbon coated α-Fe and Fe_3O_4. The carbonaceous material, which gets formed while decomposing PVA, reduces a part of Fe_3O_4 to α-Fe (metallic iron). Here the decomposition is done under vacuum. The mixture comprises porous cuboidal particles of about 5-10 microns.

[088] In the third step, 0.6 mL of 3.6 w/v % $NiSO_4$ solution is added in to 0.6 mL of 1 w/v % KOH solution, in order to obtain colloidal $Ni(OH)_2$ precipitate, which act as a pore forming agent. Then graphite-grafted active material (GGAM-15), carbon black and Bi_2S_3 are added in a proportion of 82.5:10:1 by mass in to the solution. These components are mixed homogeneously and the slurry is obtained. Then 6 w/w % polymeric binder, namely polytetrafluoroethylene (PTFE) 60 wt. % dispersion in H_2O is added. After adding PTFE in to the mixture, dough is formed. It is spread over a degreased nickel mesh of dimension 3.1×3.3 cm^2 and compacted at 675 kg/cm^2. The compressed electrodes are cured at 350°C in N_2 atmosphere for 40 minutes to obtain the negative Iron electrode. 1g of graphite-grafted active material was distributed over an area of 17.4 cm^2(graphite-grafted active material loading = 57.5 mg/cm^2). Subsequently, this negative electrode is assembled with nickel oxyhydroxide counter electrodes on either side with mercury/mercuric oxide (MMO) as a reference electrode ($E°= 0.098$ V vs. SHE) in 6 M KOH solution with 1 w/v % LiOH. Alkaline iron electrodes are subjected to galvanostatic charging and discharging at a current-density of 100 mA/g up to -0.8 V vs. MMO during the first step of discharge. A maximum specific discharge capacity of 400mAh/g is obtained at 100 mA/g current density with a faradaic efficiency of 80 % as shown in **FIG. 7**.

Example 5

[089] In the first step, 109 g of ferrous sulphate heptahydrate ($FeSO_4.7H_2O$) is dissolved in 400 mL of hot de-ionized water (about 70°C) and then 54 g of Oxalic acid dihydrate ($H_2C_2O_4.2H_2O$) is dissolved in 400 mL of hot de-ionized water (about 70°C). In order to avoid oxidation of ferrous ion in the solution by dissolved oxygen, nitrogen gas is bubbled for 10-15 minutes in to the de-ionized water prior to the experiments. Subsequently, oxalic acid solution is slowly added in to ferrous sulphate solution with continuous stirring at about 70°C and the α-ferrous oxalate dihydrate (α-$FeC_2O_4.2H_2O$) gets precipitated. The precipitated α-$FeC_2O_4.2H_2O$ is allowed for ageing along with the supernatant liquid for about 2 hrs at 70°C, allowed the precipitate to settle down, filtered and dried in air oven at 60-70°C.

[090] In the second step, 8 g of α-$FeC_2O_4.2H_2O$ and 2 g of Polyvinyl Alcohol (PVA; Mw = 1, 25,000) are extensively mixed and the resultant composite is first heated up to 200°C and maintained at that temperature for 1h for converting α-$FeC_2O_4.2H_2O$ -PVA composite to α-FeC_2O_4-PVA composite. Subsequently, the α-FeC_2O_4-PVA composite is heated to 400°C and maintained at that temperature for 1h. Finally, the temperature is raised to 600°C and maintained for 2-3 hrs to obtain graphite-grafted active material (GGAM-20), which is graphitic carbon coated α-Fe. The carbonaceous material, which gets formed while decomposing PVA, reduces the whole of Fe_3O_4 to α-Fe (metallic iron). The powder XRD pattern of graphite-grafted active material (GGAM-20) is shown in **FIG.1c**. Here the decomposition is done under vacuum. The mixture comprises porous cuboidal particles of about 5-10 microns.

[091] In the third step, 0.6 mL of 3.6 w/v % $NiSO_4$ solution is added in to 0.6 mL of 1 w/v % KOH solution, in order to obtain colloidal $Ni(OH)_2$ precipitate, which act as a pore forming agent. Then graphite-grafted active material (GGAM-20), carbon black and Bi_2S_3 are added in a proportion of 82.5:10:1 by mass in to the solution. These components are mixed homogeneously and the slurry is obtained. Then 6 w/w % polymeric binder, namely polytetrafluoroethylene (PTFE) 60 wt. % dispersion in H_2O is added. After adding PTFE in to the mixture, dough is formed. It is spread over a degreased nickel mesh of dimension 3.1×3.3 cm^2 and compacted at 675 kg/cm^2. The compressed electrodes are cured at 350°C in N_2 atmosphere for 40 minutes to obtain the negative Iron electrode. 1g of graphite-grafted active material was distributed over an area of 17.4 cm^2 (graphite-grafted active material loading = 57.5 mg/cm^2). Subsequently, this negative electrode is assembled with nickel oxyhydroxide counter electrodes on either side with mercury/mercuric oxide (MMO) as a reference electrode ($E°= 0.098$ V vs. SHE) in 6 M KOH solution with 1 w/v % LiOH. Alkaline iron electrodes are subjected to galvanostatic charging and discharging at a current density of 100 mA/g up to - 0.8 V vs. MMO during the first step of discharge. A maximum specific discharge capacity of 365 mAh/g is obtained at 100 mA/g current density with a faradaic efficiency of 73 % as shown in **FIG.7**.

[092] Therefore, the present invention provides an alkaline iron electrode for an accumulator (iron-air battery) equipped with an increased specific discharge capacity and faradaic efficiency. The alkaline iron electrode includes a synergistic combination of ingredients to impart an increased specific discharge capacity to the iron electrode.

Advantages of the present invention

[093] The present invention provides a cost-effective graphite-grafted alkaline iron electrode that is environmentally benign and which can be employed in nickel-iron and iron-air accumulators. The alkaline iron electrode renders a high specific discharge capacity and faradaic efficiency. The alkaline iron electrode of the present invention can be discharged both at high and low rates.

[094] Although the embodiments herein are described with various specific examples and process parameters, it will be obvious for a person skilled in the art to practice the embodiments herein with modifications and these modifications are deemed to be within the scope of the appended claims.

We claim:

1. A graphite-grafted alkaline iron electrode for an accumulator, comprising graphite-grafted active material with substantial amount of metallic iron(α-Fe) with an enhanced surface area, an optimum porosity and with substantially reduced amount of corresponding oxide content of iron (Fe_3O_4), an effective amount graphitic carbon derived from the organic carbon source, a conductive carbon, a faradaic efficiency agent, a metal salt and a polymeric binder.

2. The electrode of claim 1, wherein the electrode comprises approximately 80-95 w/w % of metallic iron (α-Fe), 5-20 w/w % of oxide content (Fe_3O_4), with a surface area of 10-15 m^2/g and mean pore diameter in the range of about 8-15 nm, the graphitic carbon in the range of about 2-3 w/w %, the conductive carbon in the range of about 10-20 w/w %, the faradaic efficiency agent in the range of about 1-2 w/w %, metal salt in the range of about 1-2 w/w % and at least a polymeric binder in the range of about 6-15 w/w%.

3. The electrode of claim 1, wherein the organic carbon source is selected from the group consisting of polyvinyl alcohol, resorcinol-formaldehyde resin, sucrose and starch, preferably polyvinyl alcohol.

4. The electrode of claim 1, wherein the conductive carbon is preferably carbon black.

5. The electrode of claim 1, wherein faradaic efficiency agent is selected from the group consisting of bismuth sulphide (Bi_2S_3), lead sulphide and ferrous sulphide, preferably bismuth sulphide.

6. The electrode of claim 1, wherein the metal salt is nickel sulphate.

7. A process for preparing graphite-grafted alkaline iron electrode for an accumulator, the method comprising the steps of:

preparing ferrous oxalate dihydrate (α-$FeC_2O_4.2H_2O$) from $FeSO_4.7H_2O$ and oxalic acid dihydrate;

grafting of graphite *in situ*, by decomposing ferrous oxalate dihydrate, at a temperature in the range of 550-650°C in vacuum and in the presence of an effective amount of organic carbon source;

adding faradaic efficiency agent and carbon black to the graphite-grafted active material; and

8. compacting and curing the mixture in the presence of a binder at a temperature of about 350°C, in an inert atmosphere, to obtain alkaline iron electrode having a substantial amount of metallic iron and a substantially reduced amount of oxide of iron.

9. The process of claim 7, wherein the precursor is optionally selected from group consisting of hydrated ferrous ammonium sulphate ($(NH_4)_2Fe(SO_4)_2.6H_2O$) and hydrated iron chloride ($FeCl_2.2H_2O$).

10. The process of claim 7, wherein the organic carbon source is selected from the group consisting of polyvinyl alcohol, resorcinol-formaldehyde resin, sucrose and starch, preferably polyvinyl alcohol.

11. The process of claim 7, wherein the conductive carbon is carbon black.

12. The process of claim 7, wherein faradaic efficiency agent is selected from the group consisting of bismuth sulphide (Bi_2S_3), lead sulphide and ferrous sulphide, preferably bismuth sulphide.

13. The process of claim 7, wherein the binder is selected from the group consisting of such as polytetrafluoroethylene (PTFE), polyvinylidene fluoride (PVDF), styrene-butadiene-rubber (SBR), acrylic resin, hydroxypropyl-methyl-cellulose (HPMC), neoprene latex, polyethylene (PE), poly tetrafluoroethylene-*co*-vinylidene fluoride (P(TFE-VDF)) or a mixture thereof, preferably PTFE.

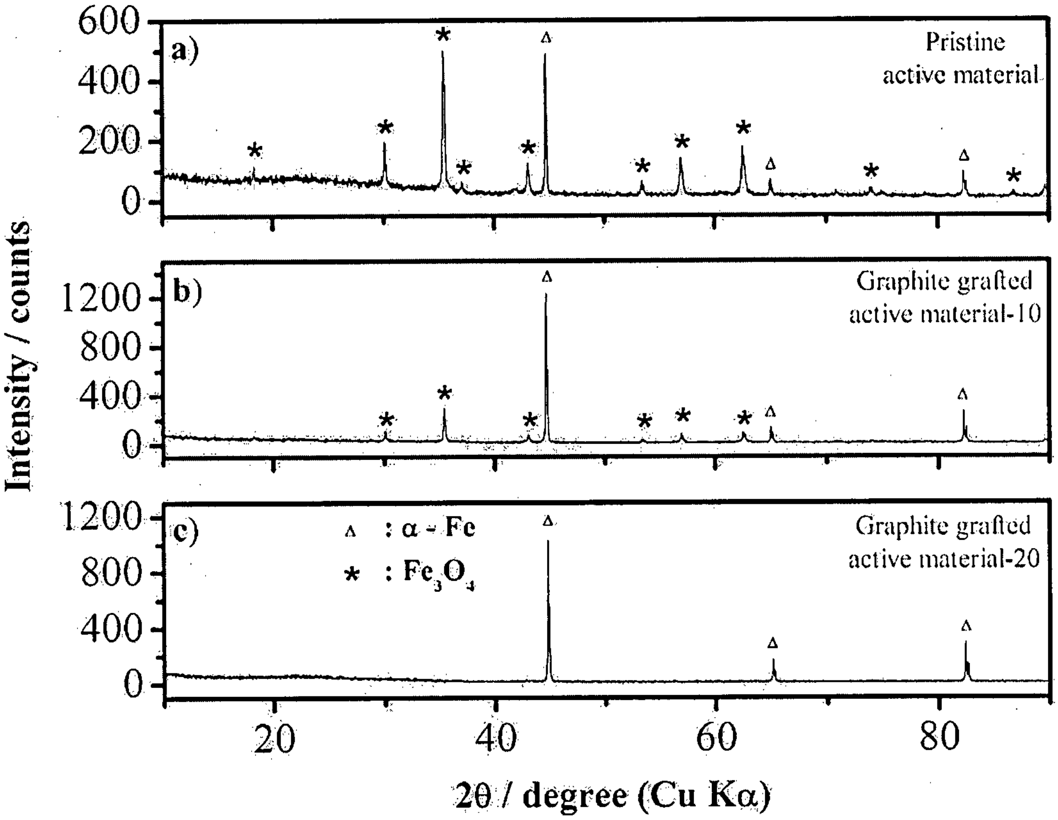
600
400
200
0
a)
Pristine active material
1200
800
400
0
b)
Graphite grafted active material-10
1200
800
400
0
c)
Graphite grafted active material-20
Δ : α - Fe
* : Fe_3O_4
Intensity / counts
20
40
60
80
2θ / degree (Cu Kα)

FIG.1

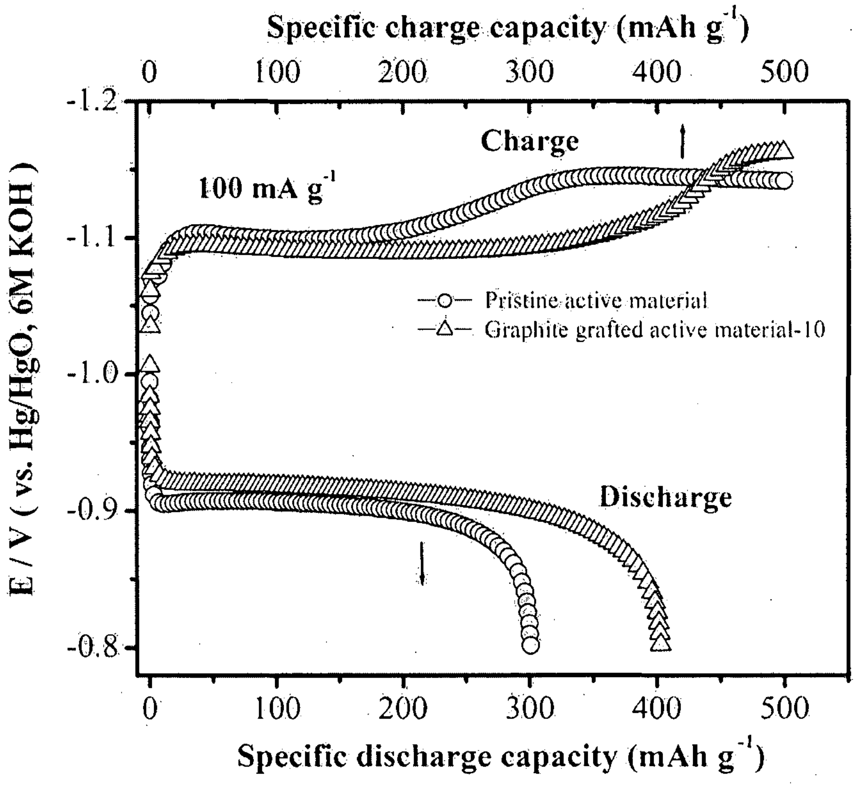
Specific charge capacity (mAh g^{-1})
0
100
200
300
400
500
-1.2
-1.1
-1.0
-0.9
-0.8
E / V (vs. Hg/HgO, 6M KOH)
Charge
100 mA g^{-1}
—○— Pristine active material
—△— Graphite grafted active material-10
Discharge
Specific discharge capacity (mAh g^{-1})

FIG.2

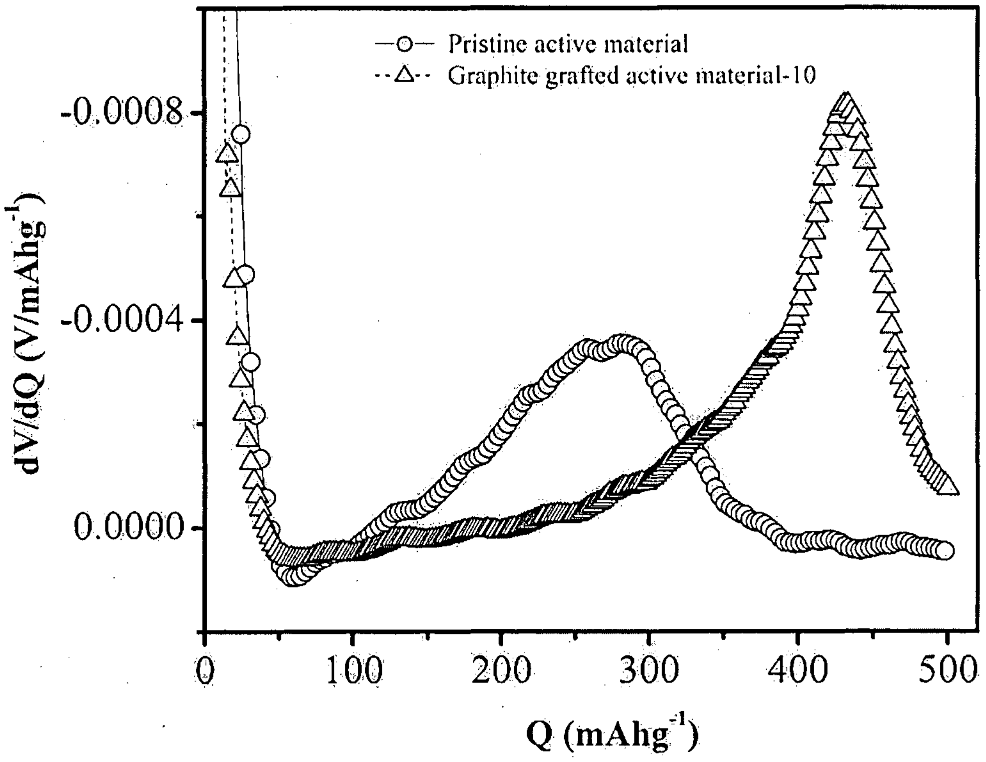
—○— Pristine active material
--△-- Graphite grafted active material-10
-0.0008
-0.0004
0.0000
dV/dQ (V/mAhg^{-1})
0
100
200
300
400
500
Q (mAhg^{-1})

FIG.3

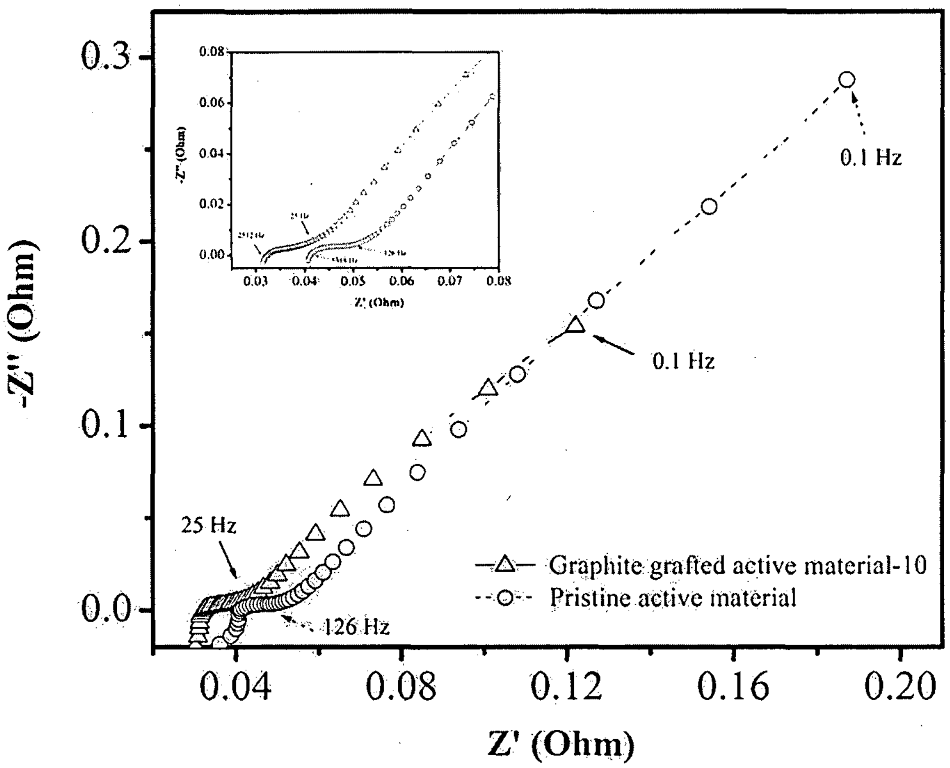
0.3
0.2
0.1
0.0
-Z'' (Ohm)
0.04
0.08
0.12
0.16
0.20
Z' (Ohm)
0.1 Hz
0.1 Hz
25 Hz
126 Hz
—△— Graphite grafted active material-10
--○-- Pristine active material
0.08
0.06
0.04
0.02
0.00
-Z'' (Ohm)
0.03
0.04
0.05
0.06
0.07
0.08
Z' (Ohm)

FIG.4

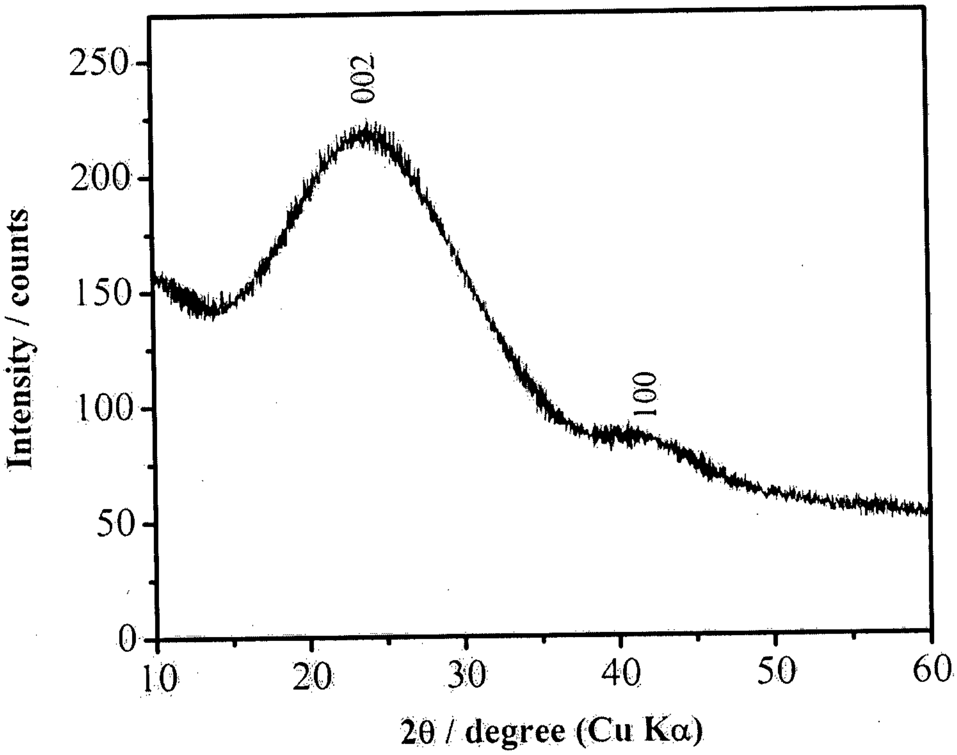
Intensity / counts
0
50
100
150
200
250
10
20
30
40
50
60
2θ / degree (Cu Kα)
002
100

FIG.5

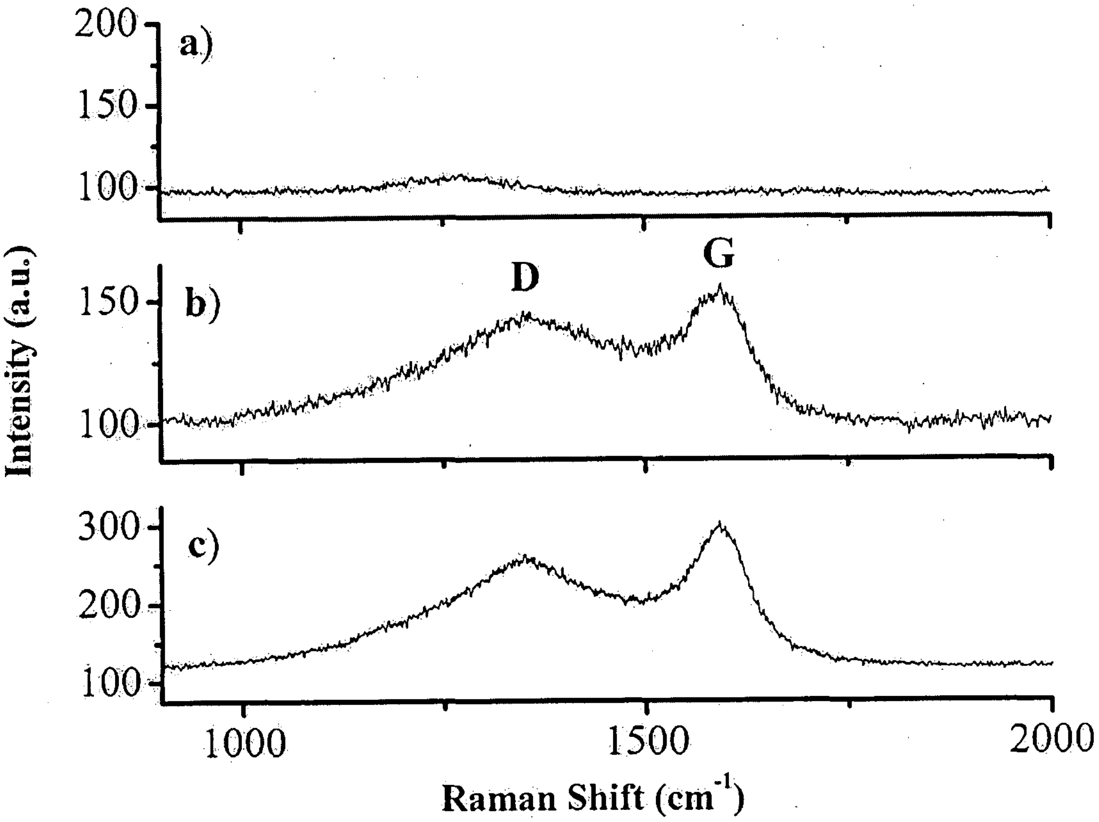
200
150
100
a)
D
G
150
100
b)
300
200
100
c)
Intensity (a.u.)
1000
1500
2000
Raman Shift (cm-1)

FIG.6

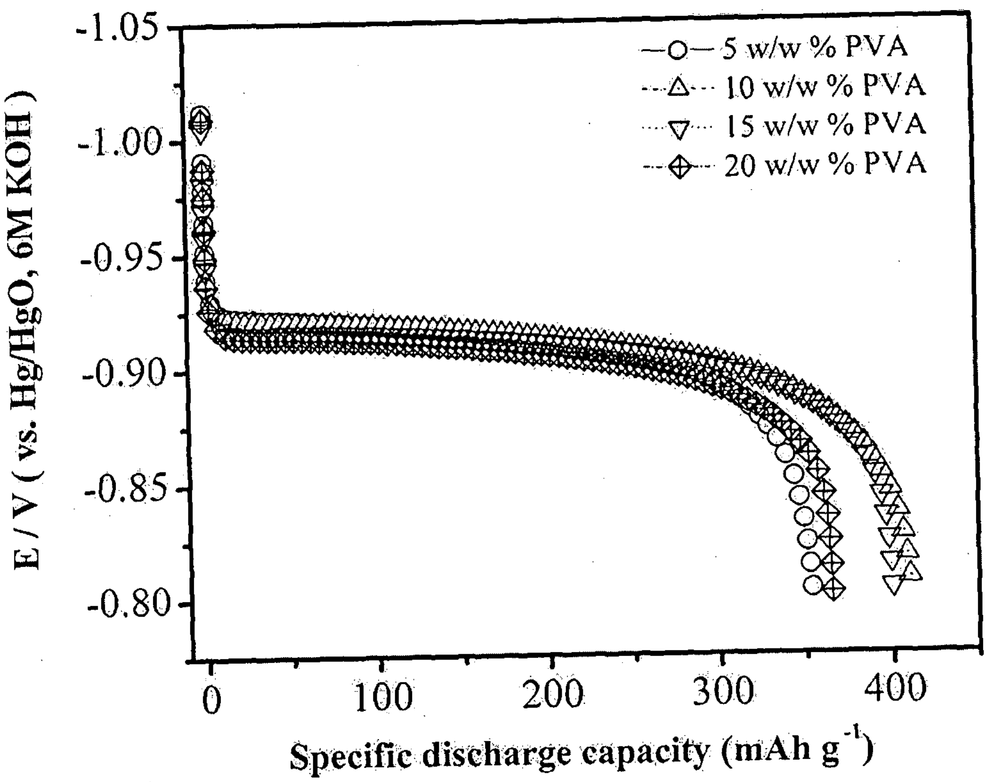
—○— 5 w/w % PVA
--△-- 10 w/w % PVA
···▽··· 15 w/w % PVA
--⊕-- 20 w/w % PVA
-1.05
-1.00
-0.95
-0.90
-0.85
-0.80
0
100
200
300
400
E / V (vs. Hg/HgO, 6M KOH)
Specific discharge capacity (mAh g^{-1})

FIG.7

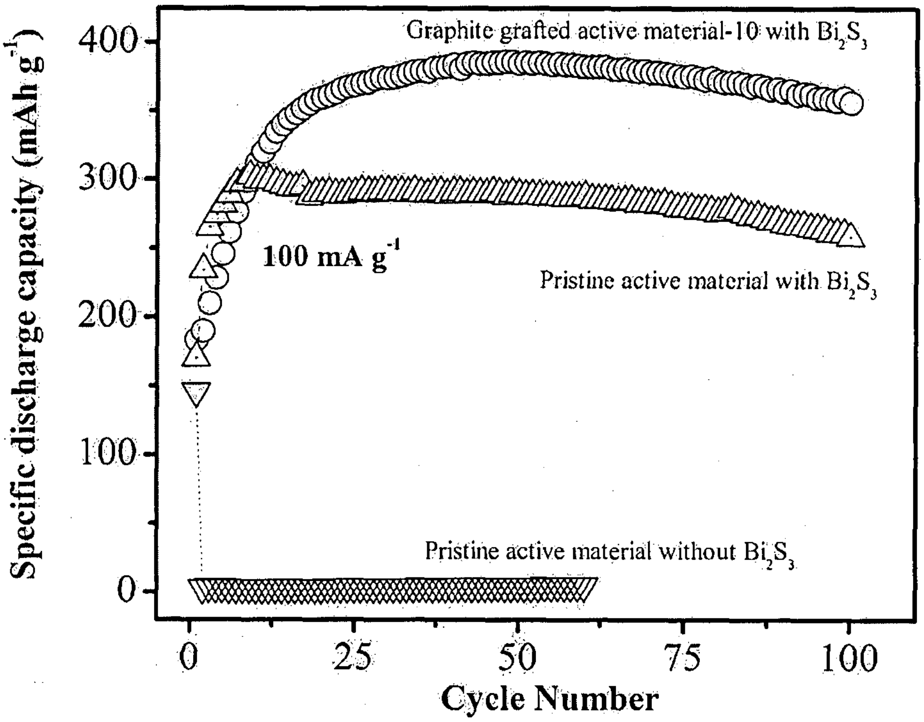
Specific discharge capacity (mAh g^{-1})
400
300
200
100
0
0
25
50
75
100
Cycle Number
Graphite grafted active material-10 with Bi_2S_3
100 mA g^{-1}
Pristine active material with Bi_2S_3
Pristine active material without Bi_2S_3

FIG.8

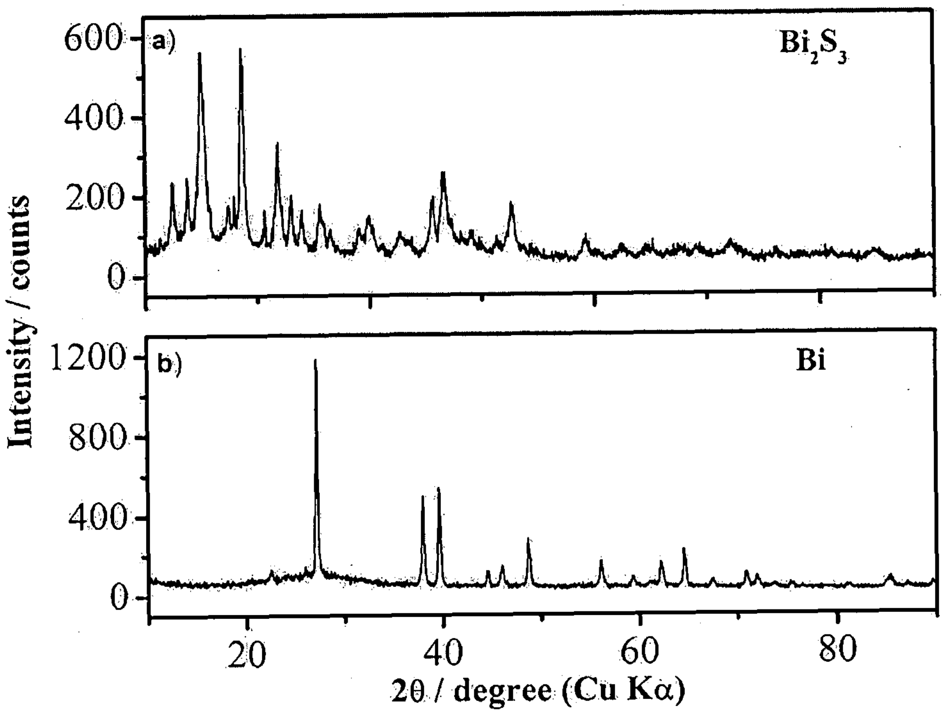
a)
Bi_2S_3
b)
Bi
600
400
200
0
1200
800
400
0
Intensity / counts
20
40
60
80
2θ / degree (Cu Kα)

FIG.9

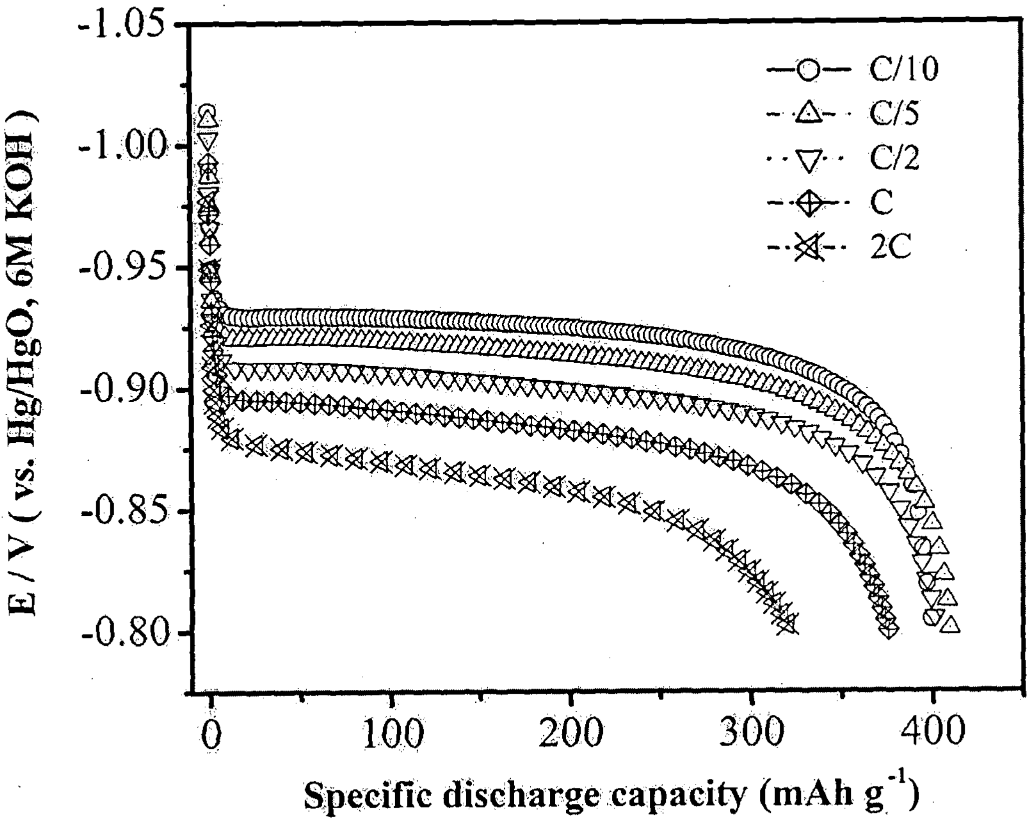
-1.05
-1.00
-0.95
-0.90
-0.85
-0.80
E / V (vs. Hg/HgO, 6M KOH)
0
100
200
300
400
Specific discharge capacity (mAh g-1)
C/10
C/5
C/2
C
2C

FIG.10

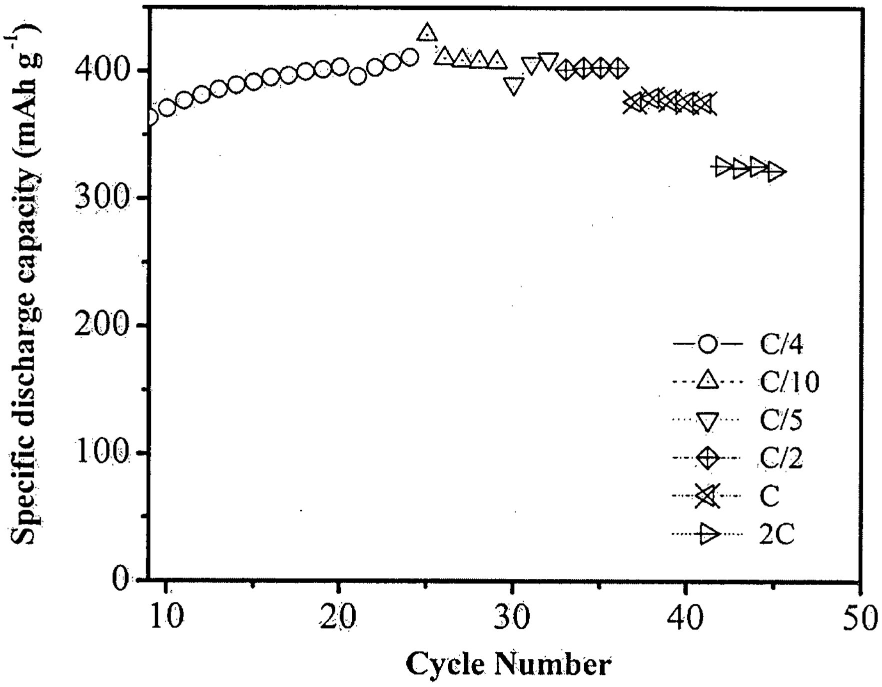
Specific discharge capacity (mAh g^{-1})
0
100
200
300
400
10
20
30
40
50
Cycle Number
C/4
C/10
C/5
C/2
C
2C

FIG.11

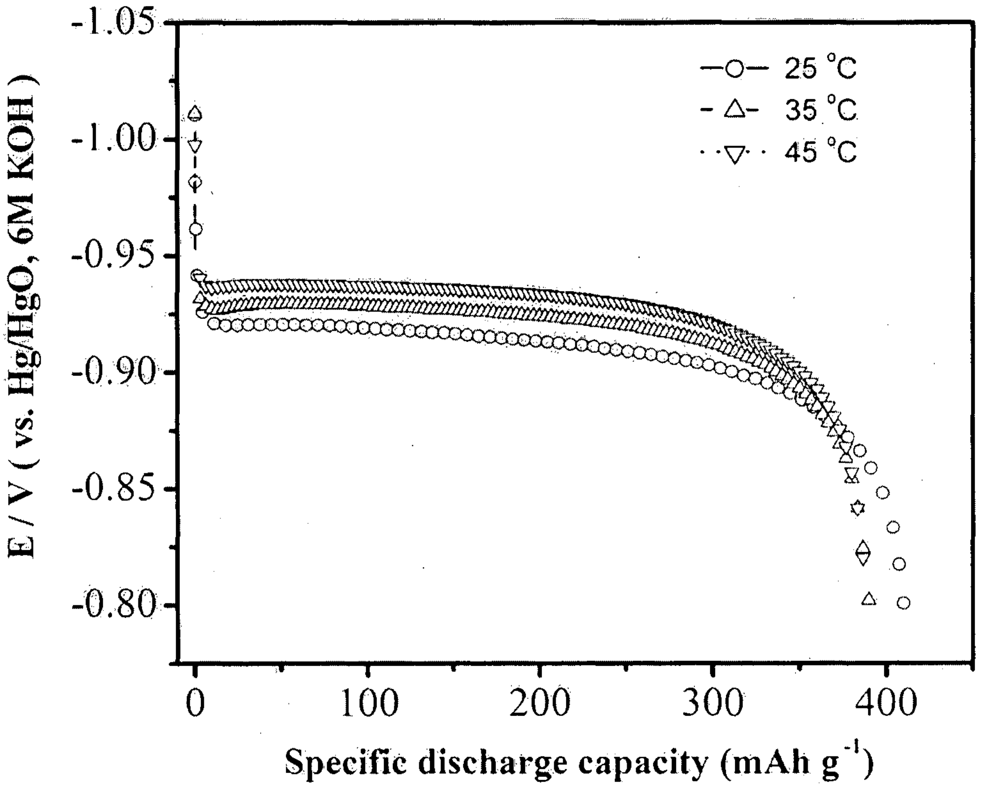
—○— 25 °C
- △- 35 °C
··▽·· 45 °C
-1.05
-1.00
-0.95
-0.90
-0.85
-0.80
E / V (vs. Hg/HgO, 6M KOH)
0
100
200
300
400
Specific discharge capacity (mAh g^{-1})

FIG.12

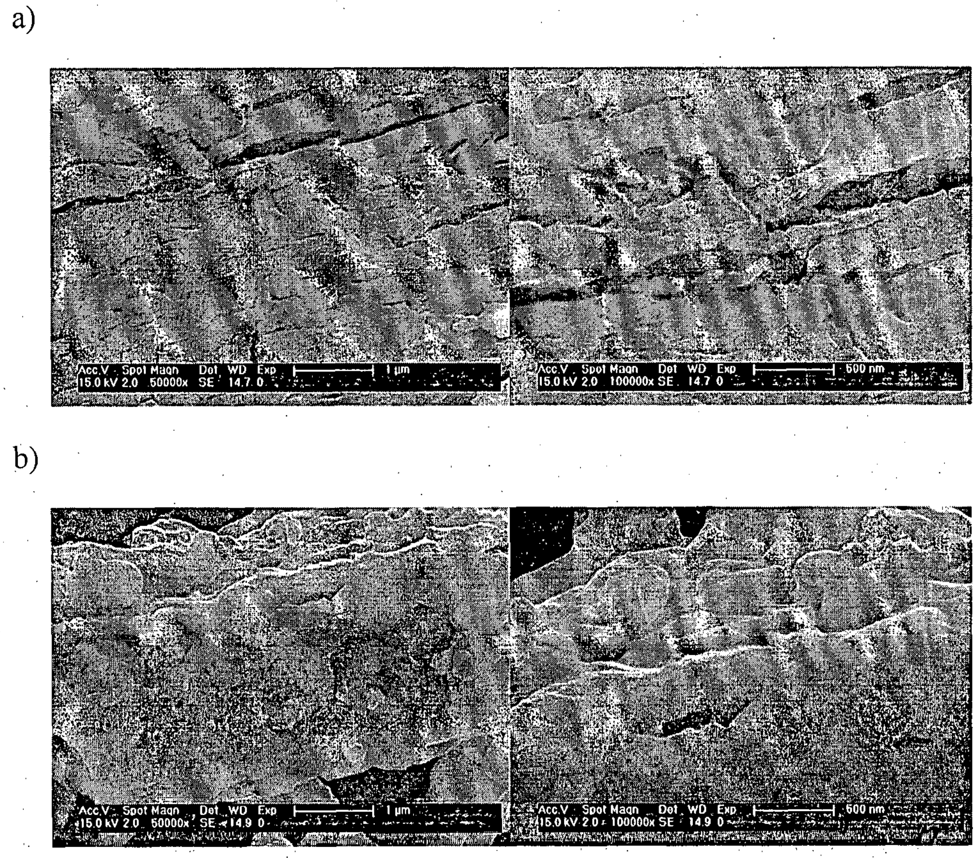
a)
Acc.V Spot Magn Det WD Exp 1 µm
15.0 kV 2.0 50000x SE 14.7 0
Acc.V Spot Magn Det WD Exp 500 nm
15.0 kV 2.0 100000x SE 14.7 0
b)
Acc.V Spot Magn Det WD Exp 1 µm
15.0 kV 2.0 50000x SE 14.9 0
Acc.V Spot Magn Det WD Exp 500 nm
15.0 kV 2.0 100000x SE 14.9 0

FIG.13

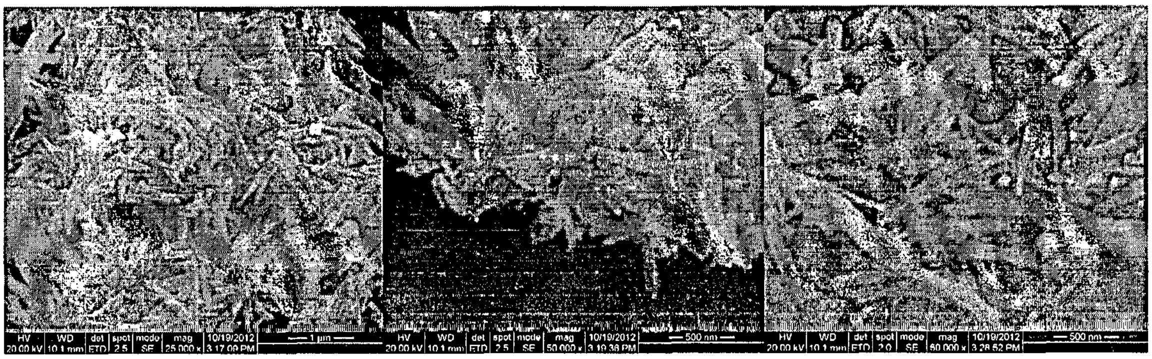
HV
20.00 kV
WD
10.1 mm
det
ETD
spot
2.5
mode
SE
mag
25 000 x
10/19/2012
3:17:09 PM
1 µm
HV
20.00 kV
WD
10.1 mm
det
ETD
spot
2.5
mode
SE
mag
50 000 x
10/19/2012
3:19:38 PM
500 nm
HV
20.00 kV
WD
10.1 mm
det
ETD
spot
2.0
mode
SE
mag
60 000 x
10/19/2012
3:28:52 PM
500 nm

FIG.14

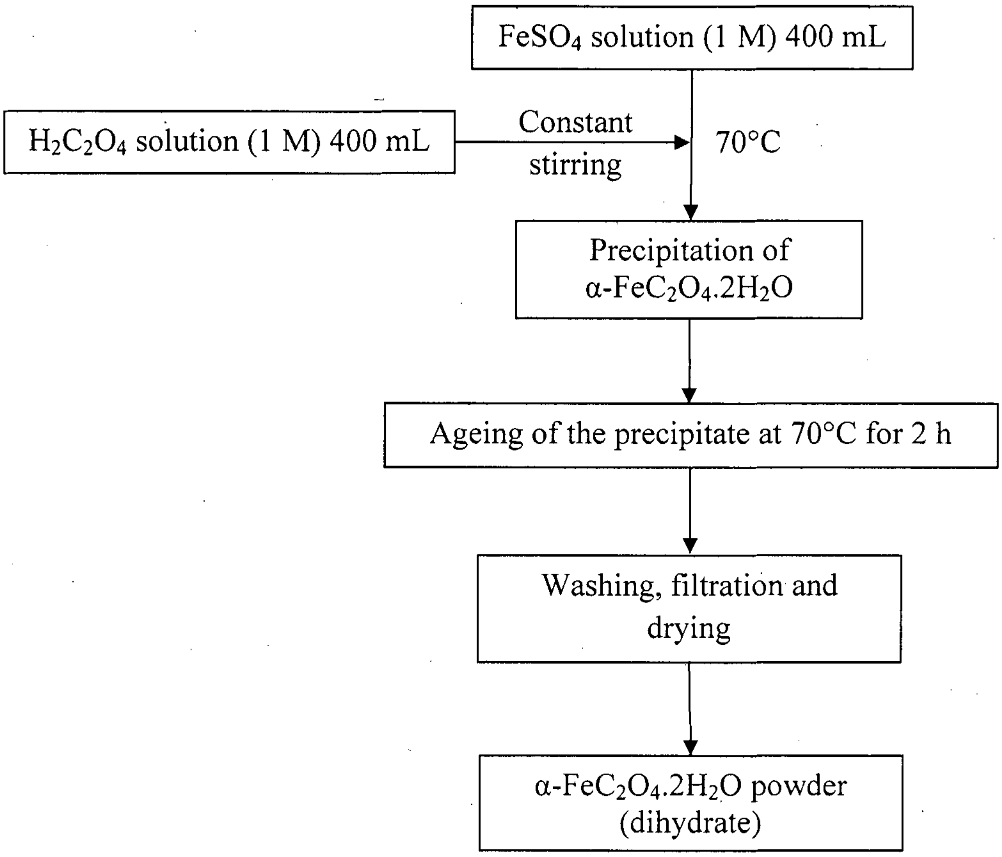
FeSO$_4$ solution (1 M) 400 mL
H$_2$C$_2$O$_4$ solution (1 M) 400 mL
Constant stirring
70°C
Precipitation of α-FeC$_2$O$_4$.2H$_2$O
Ageing of the precipitate at 70°C for 2 h
Washing, filtration and drying
α-FeC$_2$O$_4$.2H$_2$O powder (dihydrate)

FIG.15

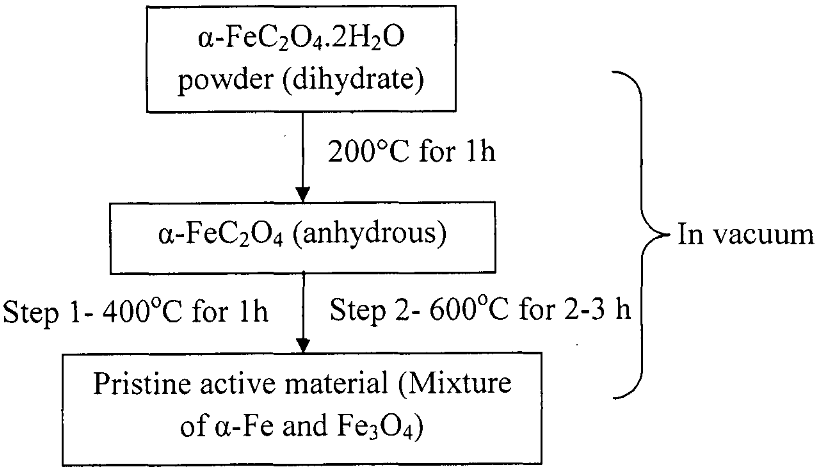
α-FeC₂O₄.2H₂O powder (dihydrate)
200°C for 1h
α-FeC₂O₄ (anhydrous)
Step 1- 400°C for 1h
Step 2- 600°C for 2-3 h
Pristine active material (Mixture of α-Fe and Fe₃O₄)
In vacuum

FIG.15

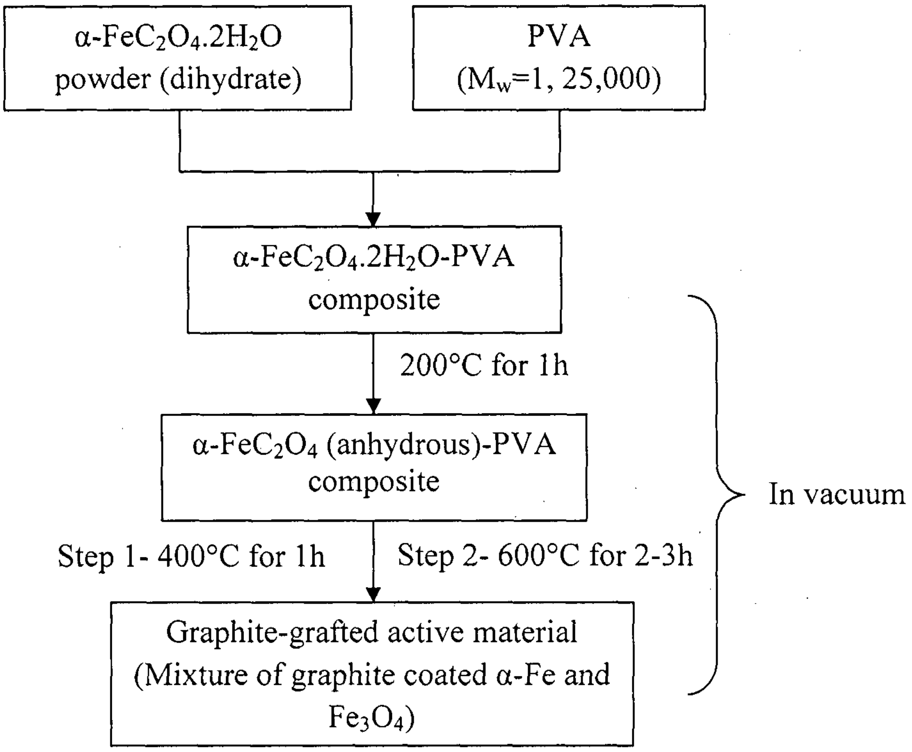
α-$FeC_2O_4.2H_2O$
powder (dihydrate)
PVA
(M_w=1, 25,000)
α-$FeC_2O_4.2H_2O$-PVA
composite
200°C for 1h
α-FeC_2O_4 (anhydrous)-PVA
composite
Step 1- 400°C for 1h
Step 2- 600°C for 2-3h
In vacuum
Graphite-grafted active material
(Mixture of graphite coated α-Fe and
Fe_3O_4)

FIG.16

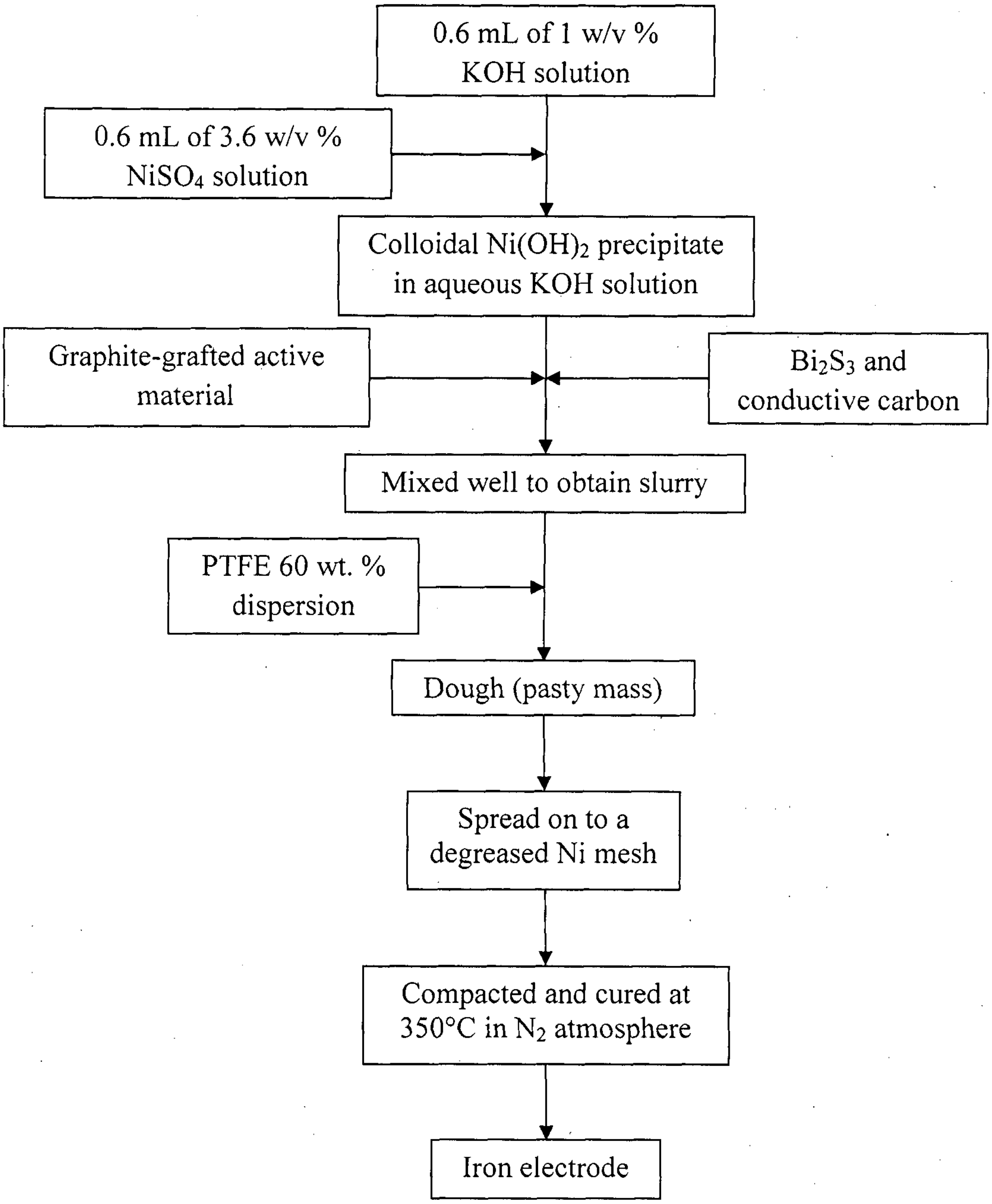
0.6 mL of 1 w/v % KOH solution
0.6 mL of 3.6 w/v % $NiSO_4$ solution
Colloidal $Ni(OH)_2$ precipitate in aqueous KOH solution
Graphite-grafted active material
Bi_2S_3 and conductive carbon
Mixed well to obtain slurry
PTFE 60 wt. % dispersion
Dough (pasty mass)
Spread on to a degreased Ni mesh
Compacted and cured at 350°C in N_2 atmosphere
Iron electrode

FIG.17

INTERNATIONAL SEARCH REPORT

International application No
PCT/IN2015/000006

A. CLASSIFICATION OF SUBJECT MATTER
INV. H01M4/24 H01M4/26 H01M4/36
ADD.

According to International Patent Classification (IPC) or to both national classification and IPC

B. FIELDS SEARCHED

Minimum documentation searched (classification system followed by classification symbols)
H01M

Documentation searched other than minimum documentation to the extent that such documents are included in the fields searched

Electronic data base consulted during the international search (name of data base and, where practicable, search terms used)

EPO-Internal, WPI Data

C. DOCUMENTS CONSIDERED TO BE RELEVANT

Category*	Citation of document, with indication, where appropriate, of the relevant passages	Relevant to claim No.
X	ARAVAMUTHAN SUNDAR RAJAN ET AL: "An in situ carbon-grafted alkaline iron electrode for iron-based accumulators", ENERGY & ENVIRONMENTAL SCIENCE, vol. 7, no. 3, 6 December 2013 (2013-12-06), pages 1110-1116, XP055189793, ISSN: 1754-5692, DOI: 10.1039/c3ee42783h abstract; passages "Experimental" and "Results and Discussion"; Fig. 2b ----- -/--	1-13

☒ Further documents are listed in the continuation of Box C.

☐ See patent family annex.

* Special categories of cited documents :

"A" document defining the general state of the art which is not considered to be of particular relevance

"E" earlier application or patent but published on or after the international filing date

"L" document which may throw doubts on priority claim(s) or which is cited to establish the publication date of another citation or other special reason (as specified)

"O" document referring to an oral disclosure, use, exhibition or other means

"P" document published prior to the international filing date but later than the priority date claimed

"T" later document published after the international filing date or priority date and not in conflict with the application but cited to understand the principle or theory underlying the invention

"X" document of particular relevance; the claimed invention cannot be considered novel or cannot be considered to involve an inventive step when the document is taken alone

"Y" document of particular relevance; the claimed invention cannot be considered to involve an inventive step when the document is combined with one or more other such documents, such combination being obvious to a person skilled in the art

"&" document member of the same patent family

Date of the actual completion of the international search

21 May 2015

Date of mailing of the international search report

29/05/2015

Name and mailing address of the ISA/

European Patent Office, P.B. 5818 Patentlaan 2
NL - 2280 HV Rijswijk
Tel. (+31-70) 340-2040,
Fax: (+31-70) 340-3016

Authorized officer

Fauché, Yann

C(Continuation). DOCUMENTS CONSIDERED TO BE RELEVANT

Category*	Citation of document, with indication, where appropriate, of the relevant passages	Relevant to claim No.
A	A Sundar Rajan ET AL: "An in situ graphite-grafted alkaline iron electrode for iron-based accumulators", Abstract #284, 224th ECS Meeting (San Francisco, California ¦ October 27 - November 1, 2013), 1 November 2013 (2013-11-01), XP055189790, Retrieved from the Internet: URL:https://ecs.confex.com/ecs/224/webprogram/Abstract/Paper22800/B1-0284.pdf [retrieved on 2015-05-18] the whole document -----	1-13
A	RAVIKUMAR M K ET AL: "A nickel-iron battery with roll-compacted iron electrodes", JOURNAL OF POWER SOURCES, ELSEVIER SA, CH, vol. 56, no. 2, 1 August 1995 (1995-08-01), pages 209-212, XP004044357, ISSN: 0378-7753, DOI: 10.1016/0378-7753(95)80037-H abstract; passage "2.1 Preparation [...] of iron negative electrodes" -----	1,7
A	GIL POSADA JORGE OMAR ET AL: "Post-hoc comparisons among iron electrode formulations based on bismuth, bismuth sulphide, iron sulphide, and potassium sulphide under strong alkaline conditions", JOURNAL OF POWER SOURCES, vol. 268, 7 July 2014 (2014-07-07), pages 810-815, XP029010631, ISSN: 0378-7753, DOI: 10.1016/J.JPOWSOUR.2014.06.126 abstract; part "2. Experimental"; Table 1 -----	1,7
A	HAILIANG WANG ET AL: "An ultrafast nickel-iron battery from strongly coupled inorganic nanoparticle/nanocarbon hybrid materials", NATURE COMMUNICATIONS, NATURE PUBLISHING GROUP, UNITED KINGDOM, vol. 3, 26 June 2012 (2012-06-26), pages 917-1, XP002729665, ISSN: 2041-1723, DOI: 10.1038/NCOMMS1921 abstract; part "FeOx/graphene hybrid as anode for ultra-Ni-Fe battery" ----- -/--	1,7

INTERNATIONAL SEARCH REPORT

International application No
PCT/IN2015/000006

C(Continuation). DOCUMENTS CONSIDERED TO BE RELEVANT

Category*	Citation of document, with indication, where appropriate, of the relevant passages	Relevant to claim No.
A	KAO C Y ET AL: "Iron/carbon-black composite nanoparticles as an iron electrode material in a paste type rechargeable alkaline battery", JOURNAL OF POWER SOURCES, ELSEVIER SA, CH, vol. 195, no. 8, 14 August 2009 (2009-08-14), pages 2399-2404, XP026807938, ISSN: 0378-7753 [retrieved on 2009-08-14] abstract; part "2. Experimental" -----	1,7